Manuscript prepared for Ann. Geophys.
with version 2.1 of the LaTeX class copernicus.cls.
Date: 7 September 2018

Characteristics of the electrojet during intense magnetic disturbances

Liudmila I. Gromova[1], Matthias Förster[2,3], Yasha I. Feldstein[1], and Patricia Ritter[2]

[1]Institute of Terrestrial Magnetism, Ionosphere, and Radiowave Propagation of the Russian Academy of Sciences (IZMIRAN), 142090 Troitsk, Moscow region, Russia
[2]Helmholtz-Centre Potsdam, GFZ German Research Centre for Geosciences, 14473 Potsdam, Germany
[3]Max-Planck-Institut für Sonnensystemforschung, 37077 Göttingen, Germany

Correspondence to: M. Förster
mfo@gfz-potsdam.de

Abstract. Hall current variations in different time sectors during six magnetic storms of the summer seasons in 2003 and 2005 are examined: three storms in the day-night meridional sector and three storms in the dawn-dusk sector. The sequence of the phenomena, their structure, positions and the strength of the polar (PE) and the auroral (AE) Hall electrojets were investigated using scalar magnetic field measurements obtained from the CHAMP satellite in accordance with the study of Ritter et al. (2004a). We analyzed the correlations of the PE and AE as well as the obtained regression relations of the magnetic latitude MLat and the electrojet current intensity I with auroral and ring current activity, the interplanetary magnetic field, and the Newell et al. (2007) coupling function for the state of the solar wind. The following typical characteristics of the electrojets were revealed:

The PE appears in the daytime sector at MLat$\sim$80°-73° with a westward or an eastward direction depending on the IMF By component (By$<$0 nT or By$>$0 nT). Changes of the current flow direction in the PE can occur repeatedly during the storm, but only due to changes of the IMF By orientation. The PE increases with the intensity of the IMF By component from I$\sim$0.4 A/m for By$\sim$0 nT up to I$\sim$1.0 A/m for By$\sim$23 nT. The MLat position of the PE does not depend on the direction and intensity of the By component.

There is no connection between MLat and I in the PE with the symmetric part of the magnetospheric ring current (index SymH). There is a correlation between I in the PE and the AsyH index, but only a very weak interconnection of this index with the MLat of the PE.

Substorms occurring during daytime before the storm main phase are accompanied by the appearance of an eastward electrojet (EE) at MLat$\sim$64°and then also of a westward electrojet (WE). In the nighttime sector, a WE appears at MLat$\sim$64°. During the main phase both electrojets persist.

The daytime EE and the nighttime WE shift toward subauroral latitudes of MLat~56°and grow in intensity up to I~1.5 A/m. The WE is then located about 6° closer to the pole than the EE during evening hours and about 2°-3° during daytime hours.

Keywords. high-latitude magnetic variations, magnetic storm phases, interplanetary magnetic field, Hall current modelling, equivalent ionospheric currents, current systems in the magnetosphere, polar electrojet, eastward and westward auroral electrojets, SymH, AsyH, AL, IndN

1 Introduction

The pioneering work of Dungey (1961) about the open nature of the magnetosphere and the role of magnetic reconnection processes between the interplanetary magnetic field (IMF) and the geomagnetic main field paved the way for the understanding of the large-scale structure and dynamics of the Earth's space environment. It provided the theoretical framework for subsequent successful investigations to understand the solar wind–magnetosphere–ionosphere–thermosphere coupling processes over several decades (Cowley, 2015).

The reconnection processes on the dayside give rise to open magnetic flux areas, the polar caps, and together with the nightside reconnections they are driving a large-scale internal magnetospheric plasma convection and current systems that connect magnetospheric and ionospheric domains. Due to the large variability of the solar wind and IMF conditions, the whole system is very dynamic and the amount of open flux in the polar cap changes continuously. The theoretical understanding of the polar cap formation and its time evolution was advanced to the fully time-dependent "expanding/contracting polar cap" (ECPC) paradigm by the work of Cowley and Lockwood (1992). A comprehensive review of all the aspects of the magnetosphere-ionosphere-thermosphere interaction processes under the solar wind driver was provided recently by Milan (2015).

The principal pattern of the large-scale field-aligned current (FAC) system, also known as Birkeland currents, which form circumpolar belts of Region-1 (on the poleward side) and Region-2 FACs (on the equatorward side) was disclosed by the work of Iijima and Potemra (1976a). On the dayside adjacent to the cusp region, so-called Region-0 FACs are observed (Iijima and Potemra, 1976b). Using MAGSAT satellite data, Iijima et al. (1984) showed in the dayside sector of the polar cap the existence of a particular FAC system, the so-called NBZ Birkeland currents for intervals of positive IMF Bz.

From ground-based magnetometer observations, the high-latitude electrojets have been studied already prior to the space era (cf., e.g., Chapman and Bartels, 1940). The particularities of high-latitude ionospheric current systems during magnetic disturbances were known empirically (Chapman, 1935). Levitin et al. (1982) revealed high-latitude current systems for summer conditions, which are controlled by the IMF components and solar wind parameters. Based on such equivalent current systems and considering informations about the anisotropic ionospheric conductivity,

Friis-Christensen et al. (1985) showed the possibility to determine a full current system, including FACs and horizontal currents in the ionosphere. Such a full current system can be estimated as a combination of the equivalent currents obtained both from ground-based and satellite observations

60 of the magnetic variations (Green et al., 2007).

An intense study of the polar electrojet (PE) at the high-latitude daytime ionosphere was initiated by the works of Svalgaard (1968) and Mansurov (1969). They had demonstrated that its characteristic magnetic field variation depends on the sector structure of the IMF that is much alike the average magnetic field of the solar photosphere. The IMF sector structure does not always correspond to the

65 expected magnetic field variations in the near-polar region. Friis-Christensen et al. (1972) showed that during periods of discrepancy between the expected magnetic variations and the sector structure from satellite observations, there existed always an essential deviation of the IMF from the usual spiral structure. During these cases, the azimuthal IMF By component was oppositely directed to the expected direction of the spiral. This implies, that the magnetic variation on ground is not primarily

70 controlled by the sector structure (toward or away the sun), but by the azimuthal component of the IMF (eastward or westward).

Various methods have been developed for the extraction of the PE magnetic field variations from groundbased observations in the near-polar region (Feldstein, 1976). The most effective approach appeared to be the correlation method (Jørgensen et al., 1972; Friis-Christensen and Wilhjelm, 1975;

75 Feldstein et al., 1975b). It is based on the fact, that both the direction of the PE and its intensity depend on the IMF By component. The method allows to separate the magnetic variations of the PE from variations of other sources and to show the spatial-temporal variation of the PE vector variations very clearly. Feldstein et al. (1975b) described the findings of a geomagnetically quiet interval in summer 1965 and the characteristics of the equivalent current system, controlled by the

80 IMF By component. In a first step, time intervals with correlations of the magnetic X(H), Y, and Z components with IMF By were identified for observatories with $\Phi > 65°$. In case of existing correlations, they appeared to be practically always close to a linear dependence with a correlation coefficient r. Correlation was assumed to exist for values of $r > 0.4$; otherwise (for $r \leq 0.4$) it was assumed as non existing. Such a boundary for significant r values is justified by the correlation

85 correction $S_r = (1 - r^2)/\sqrt{(n - 1)}$. For values of $|r/S_r| \geq 3$, the relation between the X(H), Y, and Z components with the IMF By cannot be regarded as accidental. With $n \sim 50$ the correlation is not randomly distributed for $r > 0.4$.

Regression lines, which relate the ground magnetic variations with the IMF By component, were estimated for all MLT, based on the observed intervals with $r > 0.4$. They were used to describe

90 the spatial-temporal distribution of the surface magnetic variations in the horizontal and vertical plane, and finally for the estimation of the equivalent current system for IMF By = 6nT. Its integral intensity amounts to 180 kA with a maximum current intensity of the electrojet in the dayside sector of $\sim 0.5 A/m$ at $80° < \Phi < 81°$. An analogous estimation for July-August 1966 resulted in a value

of $\sim 0.35 A/m$ at the same latitudes (Sumaruk and Feldstein, 1973).

The PE in the dayside sector does not disappear during magnetic disturbances (Feldstein et al., 2006). The PE shifts equatorward to $72° < \Phi < 74°$ in the longitudinal range of 08<MLT<17 during intense substorms (with AL$\sim$-800 nT), and during periods of geomagnetic storms with AL$\sim$-1200 nT and Dst$\sim$-150 nT it is situated at $66° < \Phi < 68°$ between 09<MLT<15. The current intensities of the PE increases only slightly to about $\sim$0.5 A/m.

The variations of the magnetic field at the Earth's surface at high latitudes, which were derived with the method of regression analysis, allowed to determine the IMF By control of the spatial-temporal distributions of the electric field potential at ionospheric altitudes as well as the ionospheric and field-aligned currents (FACs) (Friis-Christensen et al., 1985; Feldstein and Levitin, 1986). The electric field potential for an inhomogeneous ionospheric conductivity is obtained by solving a second-order partial differential equation. Friis-Christensen et al. (1985) used magnetic observations of the summer seasons in 1972 and 1973, while Feldstein and Levitin (1986) obtained it for summer 1968. The potential differences at cusp latitudes in the daytime sector are $\sim$20 kV for IMF By$\sim \pm6$ nT.

Olsen (1996) used MAGSAT magnetic field data in a height range of 350<h<550 km to determine the strength and location of the auroral electrojets at 115 km altitude. He showed for the first time the possibility to estimate the horizontal ionospheric currents from scalar magnetic measurements only. The ionospheric currents were modelled by hundreds of infinite linear currents perpendicular to the orbital plane of the spacecraft with discretisation intervals of 111 km. The problem of ionospheric current estimation is underdetermined and its solution is not unique. In order to constrain the solution, a regularization method is used. The comparison of modelled and measured variations of the magnetic field along the satellite orbit on December 04, 1979, 17:00 UT, demonstrates the good agreement for the field-aligned component, but a significant discrepancy for the field-perpendicular one. The discrepancy is mainly caused by magnetic fields of the FACs. The integral amplitude of the ionospheric currents during the interval November 28 till December 10, 1979, yielded a correlation of $r = 0.88$ with the AE-index.

The IMF By orientation influences not only the PE, but also the movements of the auroral forms at cusp latitudes (Sandholt et al., 2002). Simultaneously with permanently poleward moving discrete auroral forms at the equatorward boundary of the cusp, which are controlled by the IMF Bz component, there exist east-west moving auroral forms. This azimuthal movement is controlled by IMF By, such that for By>0 the discrete forms move westward and for By<0 eastward. The movement of the auroral forms is in opposite direction to the PE current flow direction. This can be expected, because the discrete auroral forms and the channels of enhanced ionospheric conductivity are both due to precipitating electrons into the upper atmosphere. A detailed consideration of the interrelation between auroral luminosity, auroral particle precipitation, and the PE during magnetic disturbances was given by Sandholt et al. (2004). As shown there, the strong convection channel is

located on the dawn side of the polar cap for IMF By>0, and on the dusk side for By<0 conditions. The electron precipitation in the regime of the convection channel in the morning sector consists of a band ($\sim$500 km) of structured precipitation. The PE is located on the high-latitude boundary of the structured luminosity region in the vicinity of the strong flow channel of magnetospheric convection close to the bright auroral arc. For By>0, this channel is located in the morning sector on the pole-ward side of the polar cap boundary with FAC out of the ionosphere, and FAC into the ionosphere equatorward of the polar cap boundary.

Ritter et al. (2004b) investigated variations in the location and density of the auroral electrojets, which were independently determined both from ground-based (IMAGE magnetometer network) and satellite (CHAMP) measurements. Wang et al. (2008) made use of the Hall current estimations for the intense magnetic storms of 31 March to 01 April 2001 and 17–21 April 2002 to investigate the position and current densities of auroral electrojets (WE and EE) as well as the relations of the electrojets to the Dst index and the IMF Bz component. The characteristics of the PE have not been considered by these authors. The currents were determined from scalar magnetic field measurements of the CHAMP satellite (orbit in the meridional plane of 15–03 MLT and 16–04 MLT) according to the method of Ritter et al. (2004b). The intensity of the WE on the nightside is on average two time larger than the EE on the dayside.

In this study we investigate not only the auroral electrojet, but also the polar electrojet characteristics during six intense magnetic summer storms. In section 2 we present an overview of the CHAMP data used as well as the indices, which characterize the electromagnetic conditions in the near-Earth space during the geomagnetic storms under study. Section 3 provides a short description of the method for the determination of the Hall currents from CHAMP scalar magnetic records. In section 4 we consider the latitudinal variation of the strength and position of the electrojets during different phases of the magnetic storm on 29–30 May 2003. Particular attention is drawn to the polar electrojet (PE). The subsequent section 5 provides detailed correlation analyses and the discussion of the control of the current direction in the electrojets, its strength and latitudinal position by various indices. The Conclusion's section 6 summarizes the main results of the study with respect to the Hall current variations during the various storm phases.

2   Data

The CHAllenging Minisatellite Payload (CHAMP) spacecraft (Reigber et al., 2002) was launched on 15 July 2000 into a circular, near-polar orbit with an inclination of 87.3°. From its initial orbital height at $\sim$460 km, it has decayed to $\sim$400 km in 2003 and $\sim$350 km after 5 years. The orbital plane precesses to earlier local times at a rate of about one hour per 11 days so that the orbit covers all local times within about 131 days. The data used in this study are scalar magnetic field measurements obtained with the Overhauser Magnetometer (OVM) at the boom tip with a resolution of 0.1 nT. In

Table 1. Overview of CHAMP satellite orbits used for this study.

Date & Time (UT, hrs)	CHAMP orbit numbers	MLT range (hrs)	
		ascending	decending
29/30 May 2003, 16–10	16229–16240	∼14–16	∼02–04
24 Aug 2005, 07–20	29012–29020	∼11–12	∼23–24
18 Jun 2003, 03–18	16532–16541	∼12–16	∼00–04
30 May 2005, 02–17	27658–27667	∼19–21	∼06–09
15 May 2005, 00–19	27423–27432	∼20–22	∼08–10
18 Aug 2003, 00–23	17480–17494	∼07–09	∼19–21

order to isolate the magnetic effect of ionospheric currents in the satellite data, the contributions from all other sources have been removed from the scalar field readings as described in the study of Ritter et al. (2004a).

The CHAMP orbital intervals during various storm periods used for this study are listed in Table 1.
170   The quantity, locations, and intensity of the peaks along the latitudinal current intensity distribution varies over the course of the storm development. For the description of the storm development, we utilise various solar and geomagnetic indices.

First, we employ the auroral electrojet index (AE), which is derived from geomagnetic variations in the horizontal component observed at 12 selected observatories along the auroral zone in the
175   Northern Hemisphere (http://wdc.kugi.kyoto-u.ac.jp/aedir/index.html). The upper (AU) and lower envelope (AL) of the superposed plots of all the data from these stations as functions of UT is used in this study.

Further, we employ the SymH and AsyH indices, which describe the geomagnetic disturbances at mid-latitudes in terms of longitudinally asymmetric (ASY) and symmetric (SYM) disturbances for
180   the H component (http://wdc.kugi.kyoto-u.ac.jp/aeasy/index.html or, alternatively, http://omniweb.gsfc.nasa.gov/ow_min.html). SymH is essentially the same as the Dst index, but with a different time resolution (1-min cadence).

Finally, Newell et al. (2007) proposed a new solar wind coupling function, representing the rate of magnetic flux opened at the magnetopause, $d\Phi_{MP}/dt$, which is referred to here as Index N (IndN). It is used for the correlation analysis in the solar-terrestrial physics:

$$185 \quad IndN \;=\; d\Phi_{MP}/dt \;=\; v^{4/3}B_T^{2/3}\sin^{8/3}(\theta_c/2) \tag{1}$$

Here, Φ (or Φ_{PC}) is the (open) magnetic flux that constitutes the polar cap, v describes the solar wind speed or, more precisely, the transport velocity of IMF field lines that approach the magnetopause, B_T is the magnitude of the IMF, $\sin^{8/3}(\theta_c/2)$ is the percentage of field lines, which subsequently merge, and the IMF clock angle θ_c is defined by $\theta_c = \arctan2(B_y/B_z)$. This function describes best
190   the interaction between the solar wind and the magnetosphere over a wide variety of magnetospheric activity. IndN has a strong correlation with other indices that characterize both the plasma and the

IMF in the solar wind as well as the processes in the magnetosphere. By means of a statistical study of the electrojet characteristics, the new function IndN was used together with the classical indices SymH, AsyH, and AL. For the determination of all indices throughout this study we used time averages of the overflights intervals.

3 Method

Ionospheric currents at high latitudes, which are recorded by low-Earth orbiting (LEO) satellites as magnetic field deviations, represent the sum of FACs between the magnetosphere and ionosphere (Birkeland currents) and predominantly horizontal ionospheric currents, which flow mainly in the highly conducting ionospheric E layer below the satellite orbit.

The horizontal sheet currents are commonly decomposed in two different ways. The classical fundamental theorem of vector calculus, known as Helmholtz's theorem, states that any vector field can be decomposed into the sum of a curl-free and a divergence-free part. On the other hand, considering the relation to an electric field, the sheet current is composed of Pedersen currents, which flow in the direction transverse to the magnetic field and parallel to the electric field in the neutral wind frame of reference (e.g., Baumjohann and Treumann, 1996; Richmond, 1995), and Hall currents, which are perpendicular to both fields. The latter decomposition requires, however, the knowledge of the electric field in the neutral wind frame of reference, which is not given in our case.

Using the Helmholtz theorem, we assume the Hall currents to be divergence-free, i.e., they are supposed to close entirely within the ionosphere, while the Pedersen currents are curl-free, connecting essentially various branches of FACs. Laundal et al. (2018) showed (see their Figure 14), that during summer conditions, which is the case for the six storm intervals analysed in this study, the divergence-free and curl-free ionospheric currents are mainly represented by the Hall and Pedersen currents, respectively.

The Hall current flows at high latitudes are derived from CHAMP scalar magnetometer records along the satellite orbits according to the method that was presented by Ritter et al. (2004b). This method of Hall current estimation from scalar magnetometer records of satellites was proposed for the first time by Olsen (1996). These calculations make use of a current model consisting of a series of 160 infinite current lines at an altitude of 110 km and separated by $1°$ in latitude. The magnetic field of the line currents were related to the current strength I according to the Biot-Savart law. The strength of each of the 160 line currents were derived from an inversion of the observed field residuals using a least-square fitting approach. The model does not take into account the contributions from field-aligned and Pedersen currents, measured at CHAMP altitudes. The comparison with ground-based geomagnetic variations of the horizontal component that considers only the contributions from the ionospheric Hall current field, because the contributions from the field-aligned and the Pedersen

currents largely cancel each other (Fukushima, 1976), showed the applicability with high reliability of the modelling assumptions by Ritter et al. (2004b) particularly for the estimation of the Hall currents.

230   The level of ionisation in the near noon hours at latitudes of $75° < \Phi < 80°$ decreases from summer to winter season by about an order of magnitude (Feldstein et al., 1975a). The PE current strength amounts during winter to $\sim$0.1 A/m, which makes it difficult to be measured adequately by magnetometers onboard of satellites. Because of that we investigate in this study summer storms only: three storms with CHAMP orbits in the midday-midnight plane and three in the dawn-dusk plane

235   (listed in Table 1). Here, we describe only one of these storms, namely that of May 29–30, 2003. The five other storms are described in the appendix / supplementary material to this paper.

The storm phases are identified in this study according to the SymH index, which describes together with the AsyH index the large-scale variations of the geomagnetic field with a 1-min cadence. In essence, SymH represents the mean value of the magnetic field deviation from the quiet time level

240   for a longitudinally distributed chain of six mid-latitude stations.

The intensity of the ring current varies with longitude. This variability, denoted by the AsyH index, is determined as the range between the maximum and minimum magnetic field values of the disturbance field minus the SymH from the longitudinal chain of mid-latitude stations.

4   The storm of 29–30 May 2003

245   The orbit of the CHAMP satellite in its ascending branch was on the dayside ($\sim$14–16 MLT), while its descending branch was in the nighttime sector ($\sim$02–04 MLT). Figure 1 shows various geomagnetic indices and the variation of the By and Bz components of the IMF during the storm progression together with the times of CHAMP satellite observations during crossings of the northern polar cap regions, indicated by dashed vertical lines. The respective CHAMP orbit numbers are given above

250   the uppermost panel with the first three digits on the left side and the last two digits in between the two vertical dashed lines that indicate the corresponding observation intervals.

The beginning of the main magnetic storm phase was identified during orbit 16233 at 22:24 UT with an average SymH value of -61.6 nT for the overflight interval, while the minimum value of SymH was recorded during orbit 16234 at 23:59 UT (-123.5 nT) and orbit 16235 at 01:33 UT

255   (-139.5 nT). The four orbits prior to the main phase (16229–16232) at 16:18 UT–20:53 UT are characterized by SymH values of -1.6 nT, -35.6 nT, -59.6 nT, and -27.0 nT as well as the occurence of three substorms with intensities according to AL values in the range of $\sim$-1600 nT to $\sim$-2400 nT. AsyH increases sharply prior to the beginning of the main phase (208.3 nT during orbit 16231) and during the beginning of the main phase (290.7 nT during orbit 16233). In the maximum of the main

260   phase, the values of this index decrease to 75.5 nT during orbit 16234 and 145.0 nT during orbit 16235. Following the main phase, the recovery phase develops (orbits 16236–16240) at 03:03 UT–

2003, May 29 - 30
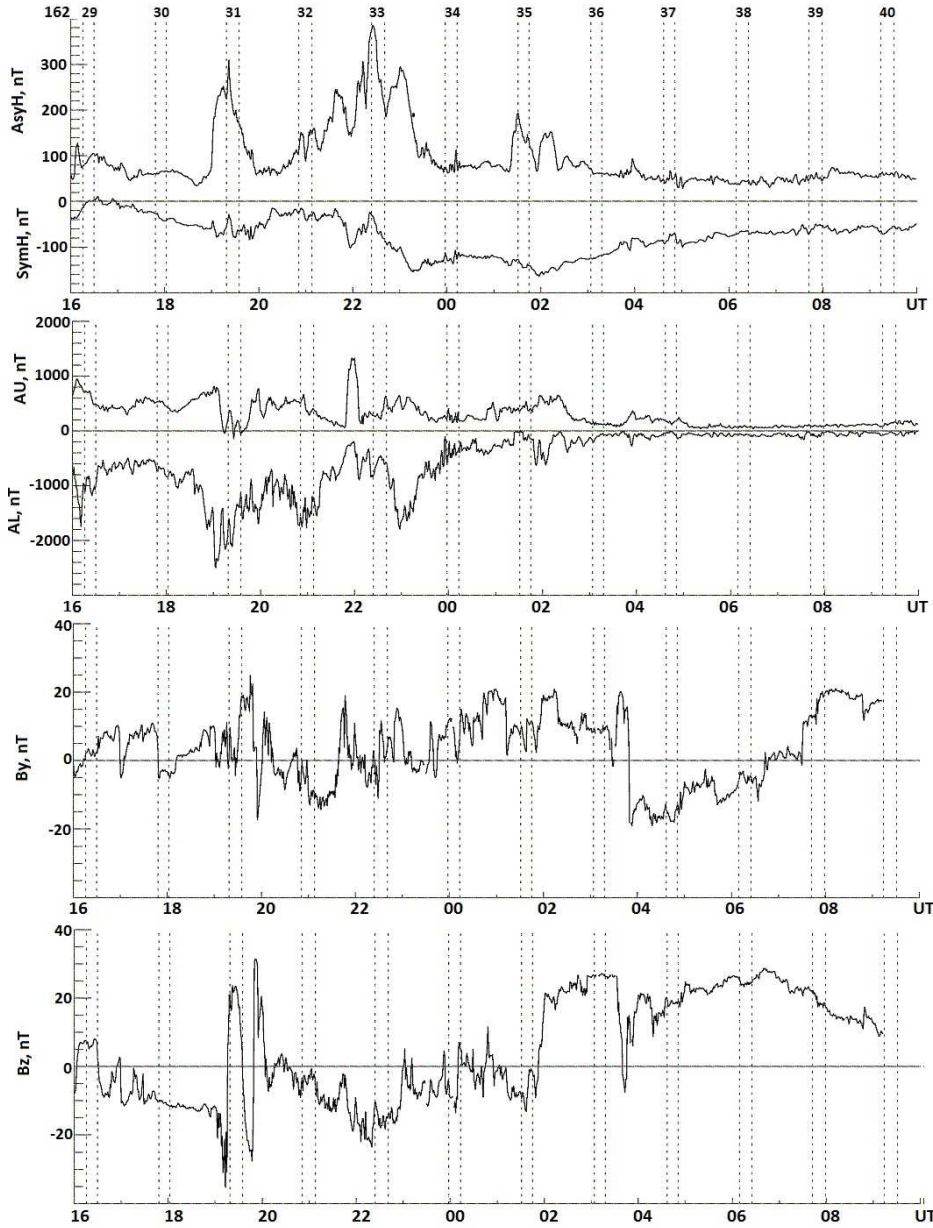
Fig. 1. One-minute values of the AsyH, SymH, AU, and AL indices and of the B_y and B_z components of the IMF for the storm of 29–30 May 2003 (analysed interval from 16:00 UT on 29 May to 10:00 UT on 30 May 2003, orbits 16229–16240). The paired vertical dashed lines indicate the UT time intervals of each satellite crossing over the northern polar cap. The orbit numbers are splitted into two parts: the two digits above the uppermost frame denote the last two digits of the orbit numbers of the CHAMP passes, while the first three digits are indicated at the upper left side.

09:21 UT, in the course of which the SymH values return to the initial values at ∼-60 nT and AsyH decreases to 51 nT during orbit 16239.

Let us now consider the structure and the latitudinal variation of the position and strength of the electrojet during the various phases of the analysed storm. The eastward (EE) and westward electrojet (WE) can exist in the daytime sector at latitudes of the auroral zone(∼60°<MLat<70°), while poleward of it, at latitudes of the auroral oval (∼73°<MLat<79°), the currents of the polar electrojet (PE) can appear. The direction of the PE, however, can be eastward or westward. This is determined by the sign of the IMF By component: eastward current in the PE for By>0, and westward for By<0. In the nighttime sector, the current is westward directed (WE) in the majority of cases at auroral latitudes. Fig. 2 shows the direction, MLat, and strength of the Hall currents along the orbit for dayside (left column) and nightside (right column) sectors as obtained from scalar measurements of the geomagnetic variations corresponding to the modelled current variations of Ritter et al. (2004b). The current direction is related to the orientation of the satellite orbit: positive currents point eastward for the descending orbital parts and westward for the ascending. The auroral electrojet current flow is assumed to be in strict east-west direction due to method constraints. It is obvious that the quantity, locations, and intensity of the peaks along the latitudinal current intensity distribution vary in the course of the storm development. A close correlation of the EE and WE can be expected for the AU and AL indices, respectively, which are regarded as a measure of the auroral electrojets from the ground. We are considering, however, magnetic records along the satellite orbit well above the ionospheric current layer.

4.1 Observations related to SymH variations

The latitudinal variation of the position and strength of the EE is shown in Fig. 2, left panels. During the orbits 16229 and 16230, one singular peak of eastward current was observed, which occurred at MLat = 63.4° and MLat = 64.0° with intensities of 1.0 A/m and 0.6 A/m, respectively. This means that the EE peak current diminishes in intensity with increasing disturbances according to the SymH index and shifts to higher latitudes. During the orbits 16231–16233 (in the substorms interval and at the beginning of the main storm phase), one can clearly note two intense peaks: one of the eastward current (EE), and another of the westward current (WE - the westward electrojet). The EE peak during orbit 16231 amounts to ∼1.83 A/m at MLat = 56.3°, decreasing in the course of the next orbit to 0.94 A/m at MLat = 63.9°.

With the beginning of the main phase, the current again intensifies to 1.61 A/m at MLat = 57.6°. The EE variations in strength and latitudinal position during the orbits 16231–16233 proceed analogeous to the SymH changes: the more intense SymH, the closer to the equator shifts the EE peak and the stronger becomes its current intensity.

But such an accordance is broken again in the maximum of the main phase similar to orbits 16234 and 16235: SymH increases in intensity, while the EE in its peak diminishes to 0.44 A/m and even

2003, May 29 - 30
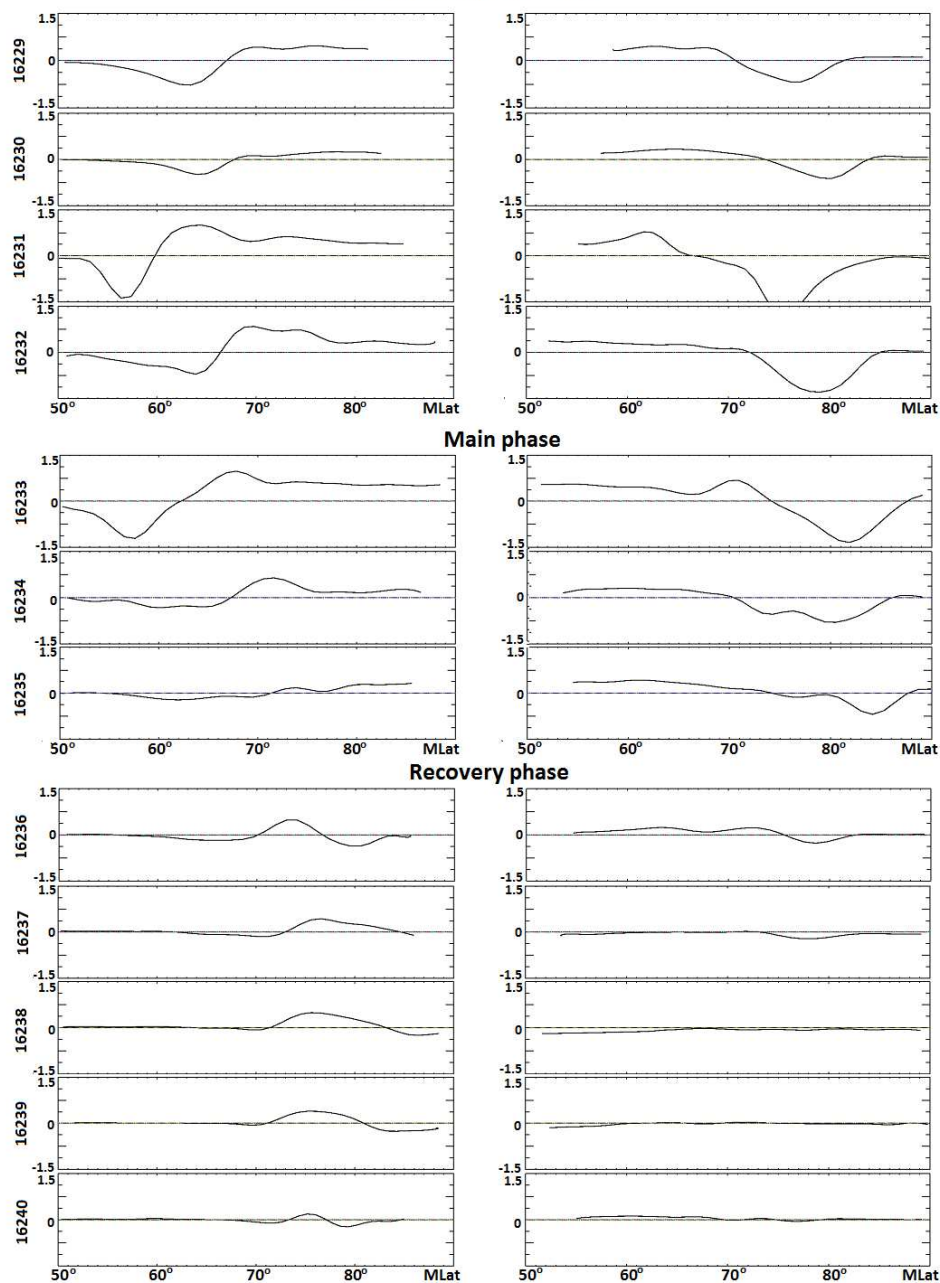
Fig. 2. Direction and intensity values of the Hall current in units of [A/m] along the satellite orbit at the dayside (left column, 14–16 MLT, corresponding to the ascending section of the orbit) and nightside sectors (right column, 02–04 MLT, descending orbit section). Positive currents denotes eastward current for the descending orbit section, and westward current for the ascending section, respectively.

0.29 A/m at MLat = 61.0°. The EE peak amounts to 0.23 A/m at MLat = 65.2° during orbit 16236 in the recovery phase and diminishes further to values <0.2 A/m during the subsequent orbits, which complicates the identification of the EE position. This way the EE follows with its varying current densities at auroral latitudes the growth (or creation) and main phases of the magnetic storm. It should be noted, that SymH remains still significant during the recovery phase, with values of ∼-60 nT. This exceeds the intensity of SymH during the substorm interval and at the beginning of the storm main phase, while the EE during the recovery phase is much smaller than during the substorm interval.

In contrast to the EE, a westward current exists on the dayside sector during the whole interval considered, except the two first orbits, and achieves during the substorm interval values of 1.1–1.3 A/m within the peaks at 64°<MLat<70°. It is obvious that the WE does not attain the CHAMP meridian (∼14–16 MLT) during the first two orbits, while it strengthens in the nighttime sector and propagates toward the evening hours. During the orbits 16231–16233, the latitude and strength of the WE peak changes in phase with the SymH intensity, analogous to the current variations in the EE peak. During the maximum of the main phase the WE peak diminishes to 0.8–0.25 A/m at 71°<MLat<74° in antiphase to SymH.

The peaks of westward current remain at a level of ∼0.6 A/m within 73°<MLat<76° during the recovery phase. An additional peak of eastward current with a strength of 0.49 A/m appears during orbit 16236 at MLat = 80.5° during early afternoon hours (MLT∼14.5 hrs). This latitude and the MLT range around midday imply that the current observed is the PE. In this case its orientation is controlled by the IMF B_y component and for an eastward PE the B_y component should be positive (Friis-Christensen et al., 1972; Sumaruk and Feldstein, 1973; Feldstein, 1976). Indeed, according to Fig. 1, B_y= 9 nT during the period of this orbit. During the two subsequent orbits, the Hall current changes its direction to westward at MLat∼80°. If this westward current prove to be the PE, then its appearance should be connected with a change of the IMF By component. Indeed, the currents are accompanied with a change of sign of the IMF B_y component, corresponding to -17.5 nT (MLat = 80.7°) during orbit 16237 and -5.2 nT (MLat =80.6°) during orbit 16238. During the orbits 16239 and 16240 the IMF B_y component turns to positive values again and weak eastward directed currents appear accordingly at MLat∼80°.

In the majority of latitudinal profiles of the nighttime sector (Figs. 2, right panels), there one peak of the WE exists at latitudes of the auroral oval and some weakly spreaded eastward currents. Two orbits constitute an exception - one prior to (16231) and another during the beginning of the main storm phase (16233). These orbits pertain to the period of intense substorms. Within the polar cap up to the geomagnetic pole, there exist quite intense (up to 0.9 A/m) eastward currents.

These currents might contain irregularities, which are caused by the appearance of a peak of eastward currents in the latitudinal profile. The monotonicity of the eastward current variations within the polar cap during most orbits provides some reason to assume, that these currents result

335   from the closure of an intense WE current, which occurs at latitudes of the auroral oval in the nighttime sector.

     At the beginning of the substorm interval (orbits 16229 and 16230) with the intensification of SymH, the WE peak shifts to lower latitudes and the current intenstiy diminishes. The most intense peaks of the nighttime WE are obtained during the substorm interval prior to the main phase

340   start with and retain values of 2.7 A/m at MLat = 64.4° (orbit 16231), 1.7 A/m at MLat = 60.9° (orbit 16232), and during the beginning of the main phase with 1.79 A/m at MLat = 58.0° (orbit 16233). Later in the maximum of the main storm phase, the WE peak current strength diminishes to 1.07 A/m at MLat = 59.5° (orbit 16234) and 0.9 A/m at MLat = 55.8° (orbit 16235). Hence, the latitudinal peaks of the WE vary during nighttime in phase with the intensification of SymH (storm

345   development) before the main phase commences at higher latitudes, while shifting to the equator during the maximum of the main phase. The peak intensities changes both in phase and in antiphase with the SymH intensity. During the recovery phase, the peak intensity of the WE current is smaller than 0.2 A/m, while the eastward currents within the polar cap are too small to be recorded.

4.2   Observations related to AsyH variations and to high-latitude currents

350   In the dayside sector during the existence of the EE (orbits 16229–16236), the peak current intensities and the peak latitude positions vary synchronous with the AsyH changes, except of one orbit (16235) during the main phase. During this orbit, the AsyH index abruptly intensifies to 145 nT with a pertaining small intensity of the EE with $\sim$0.29 A/m and a shift of MLat by $1.8°$. For the WE, the change in latitude and strenth of the peak currents is in phase with the AsyH variations

355   during the storm, with the exception of orbit 16235.

     In the nighttime sector, the intensity of the peaks and their latitude (except orbit 16235) change in phase with the AsyH variations.

4.3   Summary of the observations

Summarizing the results of Hall current observations by the CHAMP satellite during the magnetic

360   disturbance period of 29–30 May 2003 in the daytime and nighttime sectors (12–16 MLT and 00–04 MLT, respectively) we conclude:

- Intense >1 A/m eastward and westward electrojets can occur at latitudes of the auroral zone during substorm periods, which precede the magnetic storm, and during the beginning of its main phase. During the maximum of the main phase, the strength of the Hall currents as well

365   as the substorms diminish in antiphase to an increase of the SymH index.

- A fast decay of the EE and WE occurs during the recovery phase at auroral latitudes both during daytime and nighttime hours. The westward or the eastward currents can be influenced

during this storm phase by the existence of a PE at 73°<MLat<80° in the region of the dayside cusp.

370   – The direction of the current in the PE is determined by the IMF B_y component: for $B_y > 0$ the current is eastward, for $B_y < 0$ westward. The change of the current direction within the PE can occur several times during the storm development, but always in accordance with the change of the IMF B_y orientation.

  – The Hall currents in the auroral ionosphere, both the EE and the WE, vary usually in phase 375 with the SymH and AsyH variations (but sometimes also in antiphase). There are time intervals, where any correlation between the geomagnetic activity indices and the Hall current parameters is missing (see Tables 2 and 3 below in section refsec:anal). There is a closer connection of the current intensity and the MLat variations with AsyH than with SymH.

  – In the daytime sector (14–16 MLT) during a period of intense substorms, the EE is located in 380 a latitude range 56°<MLat<64°, while the WE is at 64°<MLat<70°. During the main phase of the storm, the EE shifts to 58°<MLat<62°, while the WE is situated at 64°<MLat<73°, and during the recovery phase, finally, the WE is observed at latitudes of 73°<MLat<76°. Therefore, the EE stays at about the same latitudes during the both the intense substorms and the main phase of the storm, attaining extreme equatorward values of MLat~ 56°. An 385 analogue situation exists with regard to the change of position for the WE in various storm phases, but during daytime hours the WE is located about 6° closer to the pole.

  – In the nighttime sector (02–04 MLT), there exists practically only the WE, which is located during substorms at 61°<MLat<64°, and during the main storm phase at 56°<MLat<60°. Therefore, extremal positions of the WE and EE can reach latitudes below 60°. This occurs in 390 the daytime sector for the EE, while in the nighttime for the WE.

The detailed description of the Hall current characteristics during five further magnetic summer storm intervals is transferred to the Appendix/Supplementary material.

5   Correlation analyses and discussion

In the section 4 and in the appendices A1–A5 we have investigated several geomagnetic storm peri-
395 ods, based on magnetometer measurements onboard the CHAMP satellite. The Hall currents in the high-latitude upper ionosphere of the Northern Hemisphere were analysed for various MLT sectors with regard to their position in geomagnetic latitude, their strenth and direction. The empirical description concerned the appearance of the EE, the WE, and the PE during various storm phases and was carried out primarily qualitatively.
400   Below we are going to analyse the current directions, their densities, and MLat positions for various MLT sectors with regard to solar wind parameters and some indices of the planetary magnetic

activity (SymH, AsyH, AL, IndN). We use activity indices, which characterize the occurrence and dynamics of large-scale plasma domains in Earth's magnetosphere that are responsible for the existence of concrete variations of the geomagnetic field at Earth's surface.

5.1 Polar electrojets

It is well-known from geomagnetic activity researches that the intense magnetic disturbances at the high-latitude projection of the magnetospheric cusp are not related to the occurrence and dynamics of magnetospheric substorms. Fig. 3a–f shows the correlations of the various IMF parameters and geomagnetic indices with the magnetic latitude (left side panels) and the Hall current intensity I (right side panels) obtained by CHAMP satellite crossings over the polar electrojets during 6 geomagnetic storms. The direction of the Hall currents can be distinguished in the upper panels (Fig. 3a): westward and eastward currents are indicated with blue and red data points, respectively. For the further study, we selected the electrojet parameters at their extremal values of current strength for each orbit. The data pool was augmented yet be including also neighbouring values before and after the extremal points.

Table 2. The dependent (X) and independent variable (Y), their correlation coefficients (r), the coefficients A and B of the regression equations $X = A + B * Y$, and their dispersions σ.

X	Y	r	A	B	σ
I (intensity, A/m)	By (>0)	0.59	0.535	0.018	0.160
I (intensity, A/m)	By (<0)	-0.72	0.291	-0.024	0.134
I (intensity, A/m)	$|By|$	0.56	0.433	0.018	0.170
I (intensity, A/m)	AsyH	0.74	0.396	0.004	0.138
MLat (deg)	AL	0.46	78.540	0.006	2.542
MLat (deg)	IndN	-0.52	77.750	-0.006	2.415

Fig. 3a differentiates the current measurements with regard to the azimuthal IMF component (By), i.e., between those, obtained during By>0 and those during By<0 conditions. It is clearly seen that the direction of the current within the PE is determined by the IMF By sign. For intervals with positive IMF By>0, we observe an eastward directed Hall current; for negative IMF By<0 intervals the Hall current is always westward. The current strength within the PE is correlated with the magnitude of the azimuthal IMF component By: it increases from 0.3–0.4 A/m for near-zero values to I ~0.9 A/m for $|B_y|$ ~23 nT (i.e., the maximum By value during the periods investigated). Correlation coefficients r between current intensity I and the IMF By component for By>0 and By<0 are shown in the upper right and upper left corner, respectively (Fig. 3a, right panel). The coefficients for the offset (A) and the slope (B) of the linear regression line (for $r \geq 0.46$) as well as the dispersion values σ are listed in Table 2.

The current intensity values I for $B_y \sim 0$ nT are somehow different in the regression equations for $B_y > 0$ and $B_y < 0$. Fig. 3b (right panel) shows the current intensity I as a function of the IMF component's magnitude $|B_y|$, i.e., independent of the IMF By sign. This increases the number of data points for linear regression estimation. According to this estimation, the current intensity amounts to $I \sim 0.4$ A/m for $|B_y| \approx 0$ nT, while it attains ~ 0.9 A/m for $|B_y| = 23$ nT, i.e., about twice as large. The increase of the Hall current strength within the PE can occur also in magnetically quiet intervals during the absence of magnetic activity at latitudes of the auroral zone, because such disturbances are not directly related to the IMF By component.

We could not find any essential correlation between the MLat position and the IMF By component for both $B_y > 0$ ($r = 0.04$) and $B_y < 0$ ($r = 0.32$) nor for $|B_y|$ ($r = 0.15$, see Fig. 3a and b). The current strength and its direction (eastward or westward) within the PE is controlled by the IMF By component, but the latitudinal position of the current intensity maximum does not depend on IMF By. The observed morphological peculiarity of the PE is caused by its generation mechanism. This is assumed to be due to the interaction between the magnetosphere and the supersonic plasma flow (solar wind) with a "frozen-in" magnetic field (IMF). The PE currents are generated at magnetic latitudes of the cusp due to reconnection processes between the IMF and the geomagnetic field (Jørgensen et al., 1972; Wilhjelm and Friis-Christensen, 1971). The reconnection of magnetic fields brings about a north-south electric field and an east-west Hall current at cusp latitudes in the ionosphere.

The SymH index varied during the intervals of CHAMP overflights above the polar electrojets considered in this study from -10 nT to -170 nT. As shown in Fig. 3c, there is no correlation between SymH and the MLat positions ($r = -0.13$) nor the PE current strength ($r = -0.01$). The absence of any correlation is as expected, because the current system of the DR(sym) is located completely within the magnetosphere. In case of absent FACs, it cannot serve as a source for Hall currents in the ionosphere that is responsible for the existence of PE.

According to Fig. 3d, there is a high correlation between the AsyH index and the PE current I ($r \sim 0.74$) and an absence of correlation with the MLat position of the PE ($r \sim -0.29$). The PE current strength has therefore a direct relation to the intensity of the AsyH current system: with increasing longitudinal asymmetry increases the PE current intensity, but the latitudinal position of the PE does not depend on AsyH.

A partial ring current (PRC) emerges during geomagnetic disturbances. The PRC is a westward directed current in the equatorial plane of the evening to nighttime sector at geocentric distances of R$\sim$3–4 R_E. The basic PRC current system includes Region-2 FACs into the ionosphere within this sector (Iijima and Potemra, 1976a), and an EE in the ionosphere (Feldstein et al., 2006; Kalegaev et al., 2008). Observations of fluxes of energetic neutral atoms (ENA) show increased ion fluxes in the evening-nighttime sector within the inner magnetosphere during geomagnetic disturbances, which appears to be the experimental evidence for the existence of the PRC (Kozyreva and Liemohn,

2003). A successful modeling of the PRC and the EE has been performed by Kalegaev et al. (2008)
465   for the magnetic storm event of November 06-14, 2004.

The high correlation between AsyH and the intensity of the PE gives reason to assume an IMF
By control about the characteristics of the magnetic field asymmetry inside the magnetosphere. This
component of the IMF does not directly influence the intensity of the PRC, but via the current system,
that forms by the PE with FACs between the PE and the PRC. The PRC position in the equatorial
470   plane is controlled by MLT and toward the near noon sector it shifts to the ionospheric footpoint of
the cusp region (Feldstein et al., 2006). The geocentric distance of the PRC increases therefore from
the nighttime via the evening toward earlier hours. FACs of the PRC map from inner-magnetospheric
heights to the near-cusp region, where the Hall currents flow, which are controlled by the IMF By
component. In this way forms a PRC current system, which in addition to the basic one is controlled
475   by the IMF By component.

Fig. 3e shows the correlation between the MLAT position and the strength of the PE with the
AL index of geomagnetic activity. The AL index appears to be a sensitive tracer for processes in
the central plasma sheet of the magnetospheric tail. These processes are created by injection of
energetic particles, their accumulation, and the dissipation of their energy during storm times and is
480   accompanied by changes of the boundary positions of large-scale plasma structures. They appear to
have relatively small influence on the strength and MLat position of the PE (with $r = -0.38$ and
$r = 0.46$, respectively). However, there is a distinctive tendency for the shift of the PE from $\sim$78°
to $\sim$74° with an increase of the AL index up to -900 nT.

As shown in Fig. 3f, there is a correlation of IndN with MLat in the daytime sector (r=-0.52).
485   This is obvious, because both components By and Bz are included in the definition of IndN. With
increasing IndN, the latitude of the current decreases. The correlation coefficient of IndN with the
Hall current intensity (I) is r=0.3.

To summarize, the values of the correlation coefficients r and the coefficients A and B of the
regression equations are listed in Table 2. They relate the PE current intensity and their MLat position
490   to the indices that characterize the situation in the solar wind and within the magnetosphere at the
time of the observations. They are characterized by the following peculiarities:

– The PE appears at magnetic latitudes and local times of the cusp.

– The direction of the current in the PE is controlled by the IMF By (azimuthal) component: for
By>0 the current is eastward, for By<0 the current is westward directed.

495   – The current strength in the PE increases with the intensity of the IMF By component from
I$\sim$0.4 A/m for By$\sim$0 nT up to I$\sim$1.0 A/m for By$\sim$23 nT.

– The MLat position of the PE does not depend on the orientation and the strength of the IMF
By component.

- There is no connection between MLat and the current intensity I in the PE with the magneto-spheric ring current DR (index SymH).

- There is a correlation between the current intensity I in the PE and the strength of the partial ring current in the magnetosphere (PRC, index AsyH), but practically no correlation of this index with MLat of the PE.

- The currents in the central plasma sheet appear to have a weak influence on the current intensity and the MLat position of the cusp.

- We realized a correlation between MLat and the IndN solar wind coupling function.

5.2 Auroral electrojets

The most intense Hall currents at ionospheric heights, which are responsible for the electrojets, are located at auroral latitudes in the nighttime hours. It is even there, where intense auroras occur most often in the zenith (Chapman and Bartels, 1940; Harang, 1951). These electrojets were named auroral electrojets (AE). A huge number of studies has been published on their morphology, their connections with the solar wind parameters and the plasma domains in Earth's magnetosphere, as well as on their internal processes. The AE are present during all hours of the day. Based on magnetometer data of the IMAGE and EISCAT networks, Feldstein et al. (1997) showed that the electrojets shift equatorward during the main phase of strong magnetic storms. For DST~ -300 nT, the EE in the evening and the WE in the nighttime and early morning hours shifts to $\sim 54°$–$\sim 55°$. The number of electrojets, their internal current structure, and the interconnection with the individual magnetospheric plasma domains depends both on the activity level and on the MLT position of the observation (Feldstein et al., 2006). Therefore, we consider below the results of the Hall current observations of the CHAMP satellite separately for each of the following four MLT sectors: daytime, nighttime, evening, and morning hours.

Figures 4–7 consider the MLat positions (left columns) and current densitites I (right columns) during the moments of extreme values of current strength in dependence on the SymH, AsyH, AL, and IndN indices. As in Fig. 3a, data points of electrojets with an eastward direction are indicated by red colour and those with westward direction by blue colour.

Table 3 provides the correlation coefficients r, the coefficients A and B of the linear regression equations of the type $X = A + B * Y$, which were obtained by the least-squares method with correlation coefficients $r > 0.46$, and the mean-square deviation σ from the regression line.

5.2.1 Daytime sector 09:00–14:00 MLT

The AE in the daytime sector can coexist with the PE. These two types of current can be distinguished according to the following indications (that are valid for AE in contrast to PE):

Table 3. The dependent (X) and the independent variable (Y), their correlation coefficients (r), the coefficients A and B of the regression equations $X = A + B * Y$, and their dispersions σ, listed for four different MLT intervals.

X	Y	r	A	B	σ
MLT 09:00–14:00					
MLat (WE, deg)	AsyH	-0.54	74.136	-0.052	3.89
MLat (EE, deg)	AsyH	-0.49	70.327	-0.047	3.91
MLat (EE, deg)	AL	0.68	70.192	0.005	3.28
MLat (WE, deg)	IndN	-0.74	72.215	-0.011	3.13
MLat (EE, deg)	IndN	-0.67	70.271	-0.025	3.43
MLT 14:00–21:00					
MLat (WE, deg)	SymH	0.49	72.783	0.041	4.23
MLat (EE, deg)	AsyH	-0.54	65.971	-0.036	3.67
Intensity (WE, A/m)	AsyH	0.68	0.168	0.003	0.24
Intensity (EE, A/m)	AsyH	0.64	0.217	0.004	0.29
MLat (EE, deg)	AL	0.46	64.707	0.004	3.88
Intensity (EE, A/m)	AL	-0.59	0.320	-0.001	0.31
MLT 21:00–02:00					
MLat (WE, deg)	SymH	0.53	63.806	0.032	2.25
Intensity (WE, A/m)	AsyH	0.50	0.205	0.005	0.33
Intensity (WE, A/m)	AL	-0.67	0.233	-0.001	0.28
Intensity (WE, A/m)	IndN	0.76	0.207	0.003	0.25
MLT 02:00–09:00					
MLat (WE, deg)	SymH	0.47	67.343	0.040	3.24
Intensity (WE, A/m)	AsyH	0.69	-0.089	0.010	0.38
Intensity (WE, A/m)	AL	-0.52	0.328	-0.001	0.44

1. The AE are as a rule located at MLat<73° during low geomagnetic activity conditions;

2. the Hall current direction in the AE does not depend uniquely from the orientation of the IMF By component.

Fig. 4a shows cases of AE appearance in the daytime sector with a change of the SymH index. Usually, SymH has negative values (SymH<0 nT) during geomagnetic storms. Fig. 4a shows, however, beside of the mostly negative values also some values with SymH>0. They occur as a rule during the first few hours of magnetic storms. The large scatter of the data points and their low

correlation coefficients (maximum for MLat(EE, $r = 0.39$) and I(EE, $r = 0.29$) in Fig. 4a) indicate the weak control of the AE parameters by the symmetric ring current, the index of which is SymH.

The MLat position of the AE in the daytime sector correlates with three other indices: AsyH, AL, and IndN. The AE shifts with increasing disturbances toward lower latitudes: the WE from 72° to 66°, and the EE from 70° to 57° (Fig. 4b–d). The largest correlations of MLat are found with the IndN coupling function (WE, $r = -0.74$), the smallest values for AsyH (EE, $r = -0.49$). IndN is proportional to the amount of opened magnetic flux per unit time in the polar cap, which in turn affects the current systems.

The AL and AsyH indices characterize the large-scale current systems, the magnetic fields of which influence the magnetic field configuration of the dayside sector. It should be noted that there are tendencies for the WE to be located during daytime hours a few degrees more poleward than the EE. These tendencies are clearly visible with regard to the MLat(EE and WE) positions and their relation to AsyH and IndN (Fig. 4b and d). The constant term A is in the case of AsyH 3.8° larger for the WE than for the EE, and 1.9° in the case of the solar wind coupling function IndN.

The correlation coefficients for the Hall current with the IMF By vector component and its magnitude is low (not shown). A significant correlation coefficient $|r| > 0.49$ is achieved in the daytime sector only for the MLat positions of the electrojets, while the correlation with the current densities is minimal for all indices. The electrojets can be both westward and eastward. The EE can be observed for very intense disturbances during the storm period down to MLat~57°.

5.2.2 Evening sector 14:00–21:00 MLT

Figure 5 provides data presentations in the same format as Fig. 4, but now for the evening sector. Significant correlation values r exist in the evening sector for both the current densities and the MLat positions of the electrojets. The largest values of $r \sim 0.6 - 0.7$ were obtained for current densities I, independent of the current directions (westward or eastward) in the electrojets.

There appears a dependence of MLat(WE) from the SymH index: the electrojets shifts equatorward with an increase of the ring current. The EE is located more equatorward than the WE by about ~6°. The constant term A of the regression equations amounts accordingly to MLat(EE)~66° with respect to AsyH and MLat(WE)~72° with respect to SymH.

The EE current strength exceeds those of the WE. That means, the interpretation of the EE in the evening sector as a branch-off from the WE at higher latitudes will become more unlikely (Feldstein et al., 2006).

The electrojets move more equatorward with increasing disturbance level according to any geomagnetic activity index. Their current densities rise from <0.2 A/m to 1.6 A/m for the EE, and up to 1.3 A/m for the WE. The current strength of the EE increases hence stronger than that of the WE (by about 30%). The EE is observed equatorward of MLat~60° during magnetic storm periods with the threshold latitude for the EE shift of ~53°.

575 ### 5.2.3 Midnight sector 21:00–02:00 MLT

In this sector, the WE exists almost exclusively (Fig. 6). Moreover, the current intensity correlates here well with the AsyH, AL, and IndN indices with a maximum value of $r = 0.76$ for the IndN coupling function.

The MLat(WE) position, hoewever, correlates only with the SymH index. It decreases from 62°
580 to 58° for a change of SymH from ∼-40 nT to ∼-170 nT. The lowest possible MLat appears to be ∼58°.

The WE current strength increases from values <0.2 A/m to ∼1.5 A/m for an intensification of the disturbance according to the IndN coupling function from 0 to 325, while the WE position may have an equatorward threshold value of ∼58°.

585 ### 5.2.4 Morning sector 02:00–09:00 MLT

Similar to the midnight sector, the WE exists also almost exclusively within the morning sector (Fig. 7). The current intensity correlates here well with the AsyH and AL, with a maximum value of $r = 0.69$ for the AsyH index. The WE current strength increases from values 0.32 A/m to 1.92 A/m with an increase of the AsyH value from 40 nT to 200 nT, while the electrojet position
590 moves equatorward until a threshold value of ∼56°.

The MLat(WE) position correlates only with the SymH index. In this regard the midnight and morning sectors show the same behaviour. The MLat positions are controlled predominantly by the SymH index, i.e., by the intensity of the ring current DR rather than by any other current system.

The central plasma sheet of the magnetospheric tail is the source region of the WE in the nighttime
595 sector. An increase of the DR is accompanied by a change of the geometry of the magnetic field lines that are interconnected with the central plasma sheet. This results in a shift of the ionospheric projection of the WE toward the equator. The relation between the current intensity in the WE and the AL value is not needed for the interpretation.

6   Conclusions

600 In this paper we investigated the strength and spatial-temporal distribution (versus magnetic latitude MLat and MLT) of Hall currents at high latitudes. The currents were determined from measurements of scalar magnetic field data, sampled on board the CHAMP satellite at ionospheric altitudes of ∼430 km (Ritter et al., 2004a) during a selection of six magnetic storms (see Table 1). The main findings obtained are as follows.

605 The current intensity of the PE increases with the magnitude of the IMF By component, while no correlation at all could be found between the MLat position of the PE and the IMF By component. The PE is eastward directed for IMF By>0 and westward for IMF By<0. Changes of current flow direction in the PE can occur manifold during the storm, but only due to changes of the IMF By

orientation. There is a strong correlation between the PE current strength and the extent of the ring
current asymmetry as indicated by the AsyH index, while there is no connection with the SymH
index, the symmetric part of the ring current. There is an IMF By control of the magnetic field
asymmetry inside the magnetosphere that manifests in the high correlation between AsyH and the
PE current intensity.

Auroral electrojets are located at auroral latitudes (MLat<72° during daytime hours, and MLat<68°
during nighttime) and exist during all MLT. The number of electrojets in a certain latitude range, the
structure of the currents in them, and the interconnection with concrete magnetospheric plasma do-
mains, depend on the disturbance level, which is controlled by UT as well as local time (MLT) at
the observational points. Around midnight, the WE is predominant, and it exists almost exclusively
in the morning sector. During daytime hours, the MLat positions of the auroral electrojets, both WE
and EE, correlate with the activity indices AsyH, AL, and IndN. The correlation with the current
intensities, however, is relatively small there for all indices. The largest correlations ($r \sim$0.6–0.7)
exist between the AsyH index and the current intensity of the electrojets in the evening sector.

Certain characteristic features of the electrojets appear during the different phases of a geomag-
netic storm. With the development of the main phase both the daytime EE and the nighttime WE shift
to subauroral latitudes MLat$\sim$56°, while increasing in strength up to $I \sim$1.5 A/m. During evening
hours, the WE is located by $\sim$6°closer to the pole than the EE. A splitting of the WE is possible in
the morning hours during the recovery phase, analogous to the splitting of auroral luminescence in
the auroral oval.

During evening and nighttime hours the EE displaces in the region of diffuse aurora, equatorward
of the discrete auroral forms, and projects along magnetic field lines into the inner magnetosphere
between the plasmasphere and the central plasma sheet of the magnetospheric tail (Galperin and
Feldstein, 1996). Additional to this basic term, an appreciable contribution to the EE comes during
daytime hours from the PRC, which is situated in the nearnoon sector of the equatorial magneto-
sphere near the magnetopause. The WE comprises nighttime MLT from the morning to evening
hours and is located in the central plasma sheet, projecting along the magnetic field lines into the
auroral oval. The generation of the WE takes place deep inside the plasma sheet, far from magnetic
field lines that form the polar cap boundary at the nightside. The PE is controlled by the IMF By
component and closely related to dayside reconnection processes, which cause the increase of open
magnetic flux in the polar cap.

Acknowledgements. The compilation of the storms and the corresponding IMF conditions during the inter-
vals selected was conducted by use of the one-minute OMNI data base (http://omniweb.gsfc.nasa.gov/). The
CHAMP mission was sponsored by the Space Agency of the German Aerospace Center (DLR) through funds
of the Federal Ministry of Economics and Technology, following a decision of the German Federal Parlia-
ment (grant code 50EE0944). The data retrieval and operation of the CHAMP satellite by the German Space
Operations Center (GSOC) of DLR is acknowledged.

References

Baumjohann, W. and Treumann, R. A.: Basic Space Plasma Physics, Imperial College Press, London, 1996.

Chapman, S.: The electric current systems of magnetic storms, Terr. Magn. Atmos. Elect., 40, 349–370, 1935.

Chapman, S. and Bartels, J.: Geomagnetism, 1, Geomagnetic and related phenomena, Clarendon Press, Oxford, 542p., 1940.

Cowley, S. W. H.: Dungey's Reconnection Model of the Earth's Magnetosphere: The first 40 Years, vol. 41 of Astrophysics and Space Science Proceedings, pp. 1–32, Springer International Publishing, Switzerland, doi:10.1007/978-3-319-18359-6_1, 2015.

Cowley, S. W. H. and Lockwood, M.: Excitation and decay of solar wind-driven flows in the magnetosphere-ionosphere system, Ann. Geophys., 10, 103–115, 1992.

Dungey, J. W.: Interplanetary magnetic field and the auroral zones, Phys. Rev. Lett., 6, 47–48, 1961.

Elphinstone, R. D., Murphree, J. S., and Cogger, L. L.: What is a global auroral substorm?, Rev. Geophys., 34, 169–232, 1996.

Feldstein, Y. I.: Magnetic field variations in the polar region during magnetically quiet periods and interplanetary magnetic fields, Space Sci. Rev., 18, 777–861, 1976.

Feldstein, Y. I. and Levitin, A. E.: Solar wind control of electric fields and currents in the ionosphere, J. Geomag. Geoelectr., 38, 1143–1182, 1986.

Feldstein, Y. I., Lyatskaya, A. M., Sumaruk, P. V., and Shevnina, N. F.: Ionisation of the E–layer and the variations of the magnetic field in the near-polar region (in Russian), Geomagn. Aeron., 15, 1021–1027, 1975a.

Feldstein, Y. I., Sumaruk, P., and Shevnina, N. F.: To the diagnostics of the azimuthal component of the interplanetary magnetic field, C. R. Acad. Sci. USSR, 222, 833–836, 1975b.

Feldstein, Y. I., Grafe, A., Gromova, L. I., and Popov, V. A.: Auroral electrojets during geomagnetic storms, J. Geophys. Res., 102, 14,223–14 235, doi:10.1029/97JA00577, 1997.

Feldstein, Y. I., Popov, V. A., Cumnock, J. A., Prigancova, A., Blomberg, L. G., Kozyra, J. U., Tsurutani, B. T., Gromova, L. I., and Levitin, A. E.: Auroral electrojets and boundaries of plasma domains in the magnetosphere during magnetically disturbed intervals, Ann. Geophys., 24, 2243–2276, 2006.

Friis-Christensen, E. and Wilhjelm, J.: Polar currents for different directions of the interplanetary magnetic field in the Y - Z plane, J. Geophys. Res., 80, 1248–1260, 1975.

Friis-Christensen, E., Laasen, K., Wilhjelm, J., Wilcox, J. M., Gonzales, W., and Colburn, D. S.: Critical Component of the Interplanetary Magnetic Field Responsible for Large Geomagnetic Effects in the Polar Cap, J. Geophys. Res., 77, 3371–3376, 1972.

Friis-Christensen, E., Kamide, Y., Richmond, A. D., and Matsushita, S.: Interplanetary magnetic field control of high-latitude electric fields and currents determined from Greenland magnetometer data, J. Geophys. Res., 90, 1325–1338, 1985.

Fukushima, N.: Generalized theorem for no ground magnetic effect of vertical currents connected with Pedersen currents in the uniform-conductivity ionosphere, Rep. Ionosph. Space Res. Jap., 30, 35–40, 1976.

Galperin, Y. I. and Feldstein, Y. I.: Mapping of the precipitation regions to the plasma sheet, J. Geomag. Geoelectr., 48, 857–875, 1996.

Green, D. L., Waters, C. L., Korth, H., Anderson, B. J., Ridley, A. J., and Barnes, R. J.: Technique: Large-

scale ionospheric conductance estimated from combined satellite and ground-based electromagnetic data, J. Geophys. Res., 112, doi:10.1029/2006JA012069, 2007.

Harang, L.: The Aurorae, vol. 1, Chapman & Hall, Ltd., London, The International Astrophysical Series edn., 163p., 1951.

Iijima, T. and Potemra, T. A.: The amplitude distribution of the field–aligned currents at northern high latitudes observed by TRIAD, J. Geophys. Res., 81, 2165–2174, 1976a.

Iijima, T. and Potemra, T. A.: Field–aligned currents in the dayside cusp observed by TRIAD, J. Geophys. Res., 81, 5971–5979, 1976b.

Iijima, T., Potemra, T. A., Zanetti, L. J., and Bythrow, P. F.: Large–scale Birkeland currents in the dayside polar region during strongly northward IMF: A new Birkeland current system, J. Geophys. Res., 89, 7441–7452, 1984.

Jørgensen, T. S., Friis-Christensen, E., and Wilhelm, J.: Interplanetary magnetic-field direction and high-latitude ionospheric currents, J. Geophys. Res., 77, 1976–1977, doi:10.1029/JA077i010p01976, 1972.

Kalegaev, V. V., Bakhmina, K. V., Alexeev, I. I., Belenkaya, E. S., Feldstein, Y. I., and Ganushkina, N. Y.: Asymmetry of the ring current during geomagnetic disturbances, Geomagn. Aeron. (Engl. translation), 48, 780–792, 2008.

Kozyreva, J. U. and Liemohn, M. W.: Ring current energy input and decay, Space Sci. Rev., 109, 105–131, 2003.

Laundal, K. M., Finlay, C. C., Olsen, N., and Reistad, J. P.: Solar Wind and Seasonal Influence on Ionospheric Currents From Swarm and CHAMP Measurements, J. Geophys. Res., doi:10.1029/2018JA025387, 2018.

Levitin, A. E., Afonina, R. G., Belov, B. A., and Feldstein, Y. I.: Geomagnetic variations and field-aligned currents at northern high-latitudes and their relations to solar wind parameters, Philos. Trans. Royal Soc., A304, 253–301, 1982.

Mansurov, S. M.: New evidence of the relationship between magnetic field in space and on the Earth, Geomagn. Aeron. (Engl. translation), 9, 768–773, 1969.

Milan, S. E.: Sun et Lumière: Solar wind-magnetosphere coupling as deduced from ionospheric flows and polar auroras, vol. 41 of Astrophysics and Space Science Proceedings, pp. 33–64, Springer International Publishing, Switzerland, doi:10.1007/978-3-319-18359-6_2, 2015.

Newell, P. T., Sotirelis, T., Liou, K., Meng, C.-I., and Rich, F. J.: A nearly universal solar wind-magnetosphere coupling function inferred from 10 magnetospheric state variables, J. Geophys. Res., 112, A01206, doi:10.1029/2006JA012015, 2007.

Olsen, N.: A new tool for determining ionospheric current from magnetic satellite data, Geophys. Res. Lett., 23, 3635–3638, 1996.

Reigber, C., Lühr, H., and Schwintzer, P.: CHAMP mission status, Adv. Space Res., 30, 129–134, 2002.

Richmond, A. D.: Ionospheric electrodynamics using magnetic Apex coordinates, J. Geomag. Geoelectr., 47, 191–208, 1995.

Ritter, P., Lühr, H., Maus, S., and Viljanen, A.: High-latitude ionospheric currents during very quiet times: their characteristics and predictability, Ann. Geophys., 22, 2001–2014, 2004a.

Ritter, P., Lühr, H., Viljanen, A., Amm, O., Pulkkinen, A., and Sillanpää, I.: Ionospheric currents estimated simultaneously from CHAMP satellite and IMAGE ground-based magnetic field measurements: a statistical

study at auroral latitudes, Ann. Geophys., 22, 417–430, 2004b.

Sandholt, P. E., Carlson, C., and Egeland, A.: Dayside and polar cap aurora, vol. 270 of Astrophys. Space Sci. Library, Kluwer Academ. Pub., Dordrecht/Boston/London, 287p., 2002.

Sandholt, P. E., Farrugia, C. J., and Denig, W. F.: Detailed day-side auroral morphology as a function of local time for southern IMF orientation: implications for solar wind-magnetosphere coupling, Ann. Geophys., 22, 3537–3560, 2004.

Sumaruk, P. V. and Feldstein, Y. I.: Sector structure of the interplanetary magnetic field and the magnetic variations in the near-polar region (in Russian), Kosm. Issled., 11, 155–160, 1973.

Svalgaard, L.: Sector structure of the interplanetary magnetic field and daily variation of the geomagnetic field at high latitudes, in: Geophys. Papers, R-6, Danish Meteorol. Inst., 1968.

Wang, H., Lühr, H., Ridley, A., Ritter, P., and Yu, Y.: Storm time dynamics of auroral electrojets: CHAMP observation and the Space Weather Modeling Framework comparison, Ann. Geophys., 26, 555–570, 2008.

Wilhjelm, J. and Friis-Christensen, E.: Electric field and high latitude zonal currents induced by merging of field lines, in: Geophys. Paper R-31, Dan. Meteorol. Inst., Charlottenlund, Denmark, 1971.

730

735

Appendix A Detailed description of the dynamics of further storm intervals

A1 The magnetic storm of 24 August 2005

This storm began with a sudden storm commencement (SSC) at 06:15 UT, which appeared as a jump-like increase of the SymH index up to ~30 nT. The storm phases were identified according to the 1-min values of the SymH index. Fig. A1.1 shows the magnetic activity indices SymH, AsyH, AU, AL, and the IMF components By and Bz.

The orbits 29012 and 29013 take place during the growth phase of the storm, the orbits 29014 and 29015 during the main phase, and the orbits 29016–29020 during the recovery phase. The direction and strength of the Hall currents along the orbits are shown in Fig.A1.2 during daytime hours on the left hand side corresponding to the ascending orbital sections, and on the right hand side during nighttime hours for descending orbital sections. The crossings of the auroral oval occurs between 12–13 MLT during daytime and 23–24 MLT for the nighttime column. Positive values denote an eastward current (EE) for the descending orbits, and a westward current (WE) for the ascending orbital sections.

The index values during the growth phase of the storm are in the range of 25.5–32.7 nT for SymH, 121.1–72.0 nT for AsyH, while the substorms achieve ~-1000 nT according to the AL index. SymH intensifies during the main phase up to -155.6 nT and AsyH to 206.6 nT, where intense substorms with AL ~-3000 nT occur. AsyH values decrease to 43.5 nT during the recovery phase, and we observe weakly variable SymH index values around -120 nT (see Fig. A1.1).

An EE exists during daytime hours of orbit 29012 with a current intensity of up to 1.37 A/m at MLat 72.6°. During the subsequent orbit, the eastward current intensity diminishes to 0.44 A/m at MLat 70.3°. The intensification of SymH during the main storm phase (orbit 29015) is accompanied by a continuing decrease of the eastward Hall current to 0.38 A/m at MLat=65.4°. An EE with a strength of ~0.7 A/m around midday is recorded at Mlat=57.3°, i.e., below 60°, only in connection with very intense substorms (Fig. A1.1, orbit 29014). Eastward currents at such low latitudes are missing during the other orbits of this storm period. The variations of the AsyH index reflect quite clearly the variations of the Hall current intensity: it attenuates from the orbits 29012 to 29013, and increases during orbit 29014, while it decreases again during orbit 29015.

A westward current on the daytime occurs at MLat 72°-80°, beginning with orbit 29015 and continuing until orbit 29020, i.e., throughout the recovery phase and in the absence of intense substorms. The currents achieve a maximum strength of I=1.53 A/m during orbit 29018 at MLat 76.3°. This current is controlled by IMF By>0 and changes its direction with the IMF By orientation. It is therefore definitively a PE.

The currents in the midnight sector (Fig. A1.2, right column) are generally westward directed with weak intensity. The only exception occurs during orbit 29014, where the current intensity achieves I~1.2 A/m. This orbit coincides with the development of a very intense substorm, where the Hall

current distribution is very broad with two maxima of the current intensity at MLat 61.2° and 73.0°. Such a broad latitudinal distribution of the auroral luminescence, with various maxima at different latitudes, is characteristic for the recovery phase of an auroral substorm (Elphinstone et al., 1996). But for the present storm of 24 August 2005, the broad splitting up in latitude appeared in the Hall currents during the main phase of the storm.

Summarizing the results of Hall current observations by the CHAMP satellite during the magnetic disturbance period of 24 August 2005 in the daytime and nighttime sectors (11–13 MLT and 23–24 MLT, respectively) we conclude:

For the midday sector:

– An EE with a current strength of 1.37 A/m exist during the growth phase at MLat∼73° for substorms in the auroral zone with intensities of AL∼-1000 nT.

– The EE is observed at MLat<60° during the main storm phase for intense substorms with intensities of AL∼-3000 nT.

– The variations of the EE intensities during the growth and main phases of the storm occur synchronous with the AsyH index. Comparable variations with the SymH index are not observed.

– Westward or eastward directed currents are observed during the recovery phase at 72°<MLAT<80° with a maximum intensity of ∼0.9 A/m. Their direction is controlled by the IMF By component, i.e., they are in accordance with the PE.

For the midnight sector:

– As a rule, the Hall currents are westward directed during nighttime. In the concrete observations, the WE can be splitted into several parts with several maxima versus latitude.

A2   The magnetic storm of 18 June 2003

Fig. A2.1 shows the variations of the SymH and AsyH indices for the magnetic storm of June 18th, 2003. The storm phases are represented by the orbit numbers 16532 and 16533 for the growth phase, 16534–16536 for the main phase, and 16537–16541 for the recovery phase. Extreme values of SymH and AsyH are observed during the main phase with -163 nT and 91 nT, respectively, while the substorm index AL achieves -1298 nT. The CHAMP trajectories are situated during this storm period along the meridional plane of 13–14 MLT (afternoon) and 00–02 MLT (near midnight). In the daytime sector, a EE exist during the growth phase at MLat ∼67° with I∼0.43 A/m, and a WE at MLat ∼72° with I∼0.42 A/m. Both electrojets are retained during the main storm phase with an EE of I∼0.8 A/m at MLat ∼62° and a WE of I∼0.5 A/m at MLat ∼67°. The WE only persists during the recovery phase with I∼0.3 A/m at MLat ∼78°(orbits 16537 and 16538) This high-latitude westward current near MLat ∼77°with I∼0.4 A/m does not vanish till the end of the recovery phase. Such a high-latitude position of a westward current near noontime MLT gives reason to suggest that this is

810 a polar electrojet (PE). This assumption would apply, if the IMF By component is negative. Indeed, the By component appeared to be at a steady neagative value during the orbits 16537–16541.

As a rule, the ionospheric currents in the nighttime sector are westward directed in the MLat range of 57.8°–63.0° with I∼0.5 A/m. Only during two orbits in the growth and main phases, the current strength achieved I∼(1.1–1.4) A/m.

815 It should be noted that this storm had relatively intense SymH values, while the AsyH values remained however at a relatively low level. The EE and WE intensities were small as well.

Summarizing the results of Hall current observations by the CHAMP satellite during the magnetic disturbance period of 18 June 2003 in the daytime and nighttime sectors (13–14 MLT and 00–02 MLT, respectively) we conclude:

820 – The quite strong geomagnetic storm (according to the SymH<-150 nT index value during the main phase) is accompanied by substorms with AL up to -1500 nT and with the uppermost index value for the asymmetry of the field AsyH<100 nT. The peculiarities of this storm period caused obviously the appearance of an EE in the daytime sector and a WE in the nighttime sector at MLat<60°.

825 – A stable PE with a current intensity up to 0.4 A/m in westward direction persists during the recovery phase with an IMF By<0 nT component.

A3 The magnetic storm of 30 May 2005

Fig. A3.1 shows the variations of the SymH, AsyH, AU, and AL indices for the magnetic storm of May 30, 2005, between 02 UT and 20 UT. The vertical dotted lines indicate the time intervals of
830 the satellite crossings over high latitudes of the Northern Hemisphere (MLat>60°), and the numbers denote the satellite's orbit counter. Prior to the storm onset (orbits 27659 and 27660), the geomagnetic field is according to all indices, including the AL index, relatively quiet. It is recovered from -28.6 nT to -17.3 nT in terms of SymH, from 37.8 nT to 17.8 nT for AsyH, and from -40 nT to 0 nT with respect to the AL index. These changes correspond to a recovery process toward a quiet
835 time level after the previous disturbance.

The main phase of the magnetic storm starts with a steady increase of SymH from -28.6 nT during orbit 27661, a jump-like increase from 44.5 nT to 104.2 nT in AsyH during the same overflight and continues with a decrease of SymH to -118.4 nT during orbit 27665. The peak values of AsyH and AL during the main storm phase are 162.1 nT and -1200 nT, respectively. The recovery phase
840 takes place during the orbits 27666 and 27667, after which during the orbit 27668 the appearance of a new disturbance is recorded (according to the AL and SymH indices). The ascending CHAMP trajectory during the storm goes along the 19–21 MLT meridian (evening), while the descending orbit section is along the 06–09 MLT meridian in the morning sector. Fig. A3.2 shows the direction and the strength of the Hall currents for the evening (left side) and morning (right side) sectors.

845   During the orbits prior to the beginning of the main phase, the Hall current is either missing in the evening sector or exists only in terms of a distributed eastward current with maximum densities of J∼0.3 A/m at MLat∼66°. In the morning sector, a WE is recorded with J∼0.9 A/m at MLat∼80° and MLT∼09 hours. The existence of such intense currents during daytime hours at such high latitudes during relatively quiet geomagnetic conditions is unusual. A reasonable explanation might be the

850   assumption that this current concerns the PE. In this case, the orbits investigated should occur during conditions of IMF By<0 nT. Indeed, according to Fig. A3.1 a quite stable negative IMF By∼-18 nT is observerd prior to the main storm phase The beginning of the main phase (orbit 27661) is characterized by the appearance of two currents in the evening sector: the EE with J∼0.6 A/m at MLat∼63° and the WE with J∼0.3 A/m at MLat∼68°. In the course of the storm, the EE attains

855   a strength of J∼0.7 A/m, shifting equatorward until MLat∼80°. The displacement in MLat toward the equator reflects the more general tendency, according to which the the electrojets move more equatorward with increasing current J. The current intensity in the WE retains at J∼0.4 A/m. In the morning sector, the current stays at MLat∼70°, and its current strength during orbit 27661 is kept at J∼0.4 A/m. This is obviously the first appearance of an auroral WE in the morning sector. The WE

860   at auroral latitudes increases during the subsequent orbits and attains 1.5 A/m during orbit 27665 at MLat∼64°. The recovery phase during orbit 27667 is characterized by a westward current with J∼-1.0 A/m in the morning sector at MLat∼68° and a weaker current with J∼0.3 A/m at MLat∼63°,. In the course of the storm, the current intensity J in the morning sector exceeds significantly the Hall current intensity values of the same orbit in the evening sector.

865   Summarizing the results of Hall current observations by the CHAMP satellite during the magnetic disturbance period of 30 May 2005 in the dusk and dawn sectors (19–21 MLT and 06–09 MLT, respectively) we conclude:

    – Two auroral Hall currents (EE and WE) exist in the evening, and one current only (WE) in the morning sector;

870   – The currents are positioned, as a rule, at latitudes MLat of the auroral zone (63°-68°). During the main phase, the current can be shifted to MLat∼58.5°;

    – In the evening sector, the position of the EE is more equatorward than the WE;

    – During early evening hours, the Hall current strength of the EE exceeds the WE current intensity, and in the morning hours the WE current intensity is larger than during the evening;

875   – The recovery process toward the quiet-time level can be accompanied at by late evening or polar electrojet (PE) at MLat∼80° in the late morning hours of the PE with J∼0.8 A/m.

A4   The magnetic storm of 15 May 2005

Fig. A4.1 shows the variations of the SymH, AsyH, and IndN indices, as well as the IMF By and Bz components and the solar wind velocity in the interval 00–23 UT for the magnetic storm of May
880   15, 2005. The main phase of the magnetic storm takes place during the orbits 27426 and 27427 with a SymH index value of -274.5 nT, an AsyH of 186.1 nT, and AL sim-1700 nT. The orbits 27423 and 27424 prior to the main phase occur during weakly disturbed magnetic field conditions with SymH ∼50 nT and AsyH ∼75–16 nT. During orbit 27425 with SymH 48.8 nT, the AsyH index increases strongly to 121.3 nT, which appears to be the onset of an intense magnetic storm.
885   The recovery phase takes place during the orbits 27428 and 27432, during which occurs a steady decrease of the SymH index to -125.2 nT and of the AsyH index value to 70.1 nT. The ascending CHAMP trajectory during the storm spread along the 20–22 MLT meridian, and the descending trajectory is along the 08–10 MLT meridian in the morning sector. Fig. A4.2 shows the direction and the strength of the Hall currents for the evening (left side) and morning (right side) sectors.
890   The current strength for the EE during orbit 27425 is with ∼0.4 A/m quite small in the evening sector prior to the main phase. Both an EE and a WE exist during the main phase with J∼0.6 A/m. The EE shifts on average to a MLat of ∼52.5° with SymH ∼-250 nT. The Hall currents are practically absent during the recovery phase.

In the evening sector, the currents turn out to have difficult characteristics, changing with the storm
895   phases. A WE at MLat∼72° with J∼1.0 A/m is recorded during the magnetically quiet period prior to the main phase. With the development of the main phase, the WE shifts to MLat∼61°. During the recovery phase, the WE decays at auroral latitudes, but in the latitudinal range 77°<Mlat<80° an EE appears with J∼1.0 A/m (orbits 27428–27431). The orbits with an EE coincide temporally with an interval of IMF By>0 nT in the solar wind (Fig. A4.1). All characteristic features of the PE
900   are therefore present here. During orbit 27433, the direction of the current changes to WE. This is accompanied by a corresponding change of the IMF By orientation as can be seen in Fig. A4.1.

The characteristic features of this storm are the following:

– The quiet-time level of the magnetic field variations prior to the storm main phase can be describes as missing or unimportant intensities of the EE and WE Hall currents in the evening
905   sector, while in the morning sector exists only the WE at auroral latitudes.

– During the main phase of this intense storm with a SymH index of ∼-250 nT in the evening sector, the WE shifts to MLat∼52.5°, and the WE to MLat∼54.0°.

– A PE appears during the recovery phase in the late morning hours at 77°<Mlat<80°, where the Hall currents are controlled by the direction of the IMF By component.

910 ## A5 The magnetic storm of 18 August 2003

Fig. A5.1 shows the variations of the SymH, AsyH, AU, and AL indices, as well as the IMF By and Bz components in the interval 00–23 UT for the magnetic storm of August 18, 2003. The main phase of the magnetic storm takes place during the orbits 17482–17489 with peak values of SymH and AsyH of -133.8 nT and 101.4 nT, respectively, and an AL value of sim-1400 nT. During

915 the orbits 17480 and 17481 prior to the main phase the values of SymH and AsyH are -18.4 nT to -43.3 nT and 72.0–48.8 nT, and during the recovery phase in the course of orbits 17490–17493 they amount to 115.4 nT and 56.7 nT, respectively. The CHAMP trajectories during the storm spread along the 07–09 MLT meridian (morning) and along the 19–21 MLT meridian(evening). Fig. A5.2 shows the direction and the strength of the Hall currents for the morning (left side) and evening (right

920 side) sectors.

The characteristic peculiarities of the spatial-temporal distribution of the FACs during this storm concur with those described for the other storms. During the main phase in the evening sector, there exists, as a rule, an EE. The EE appears at MLat$\sim$66.5° with J$\sim$0.6 A/m, and shifts then equatorward to MLat$\sim$58.8° with J$\sim$1.0 A/m during orbit 17486. A WE exists in the morning sector at auroral

925 latitudes of 61°<Mlat<65°with J$\sim$1.2 A/m. A weak distributed eastward current in the polar cap persists due to the closure of parts of the electrojets across the near-polar region.
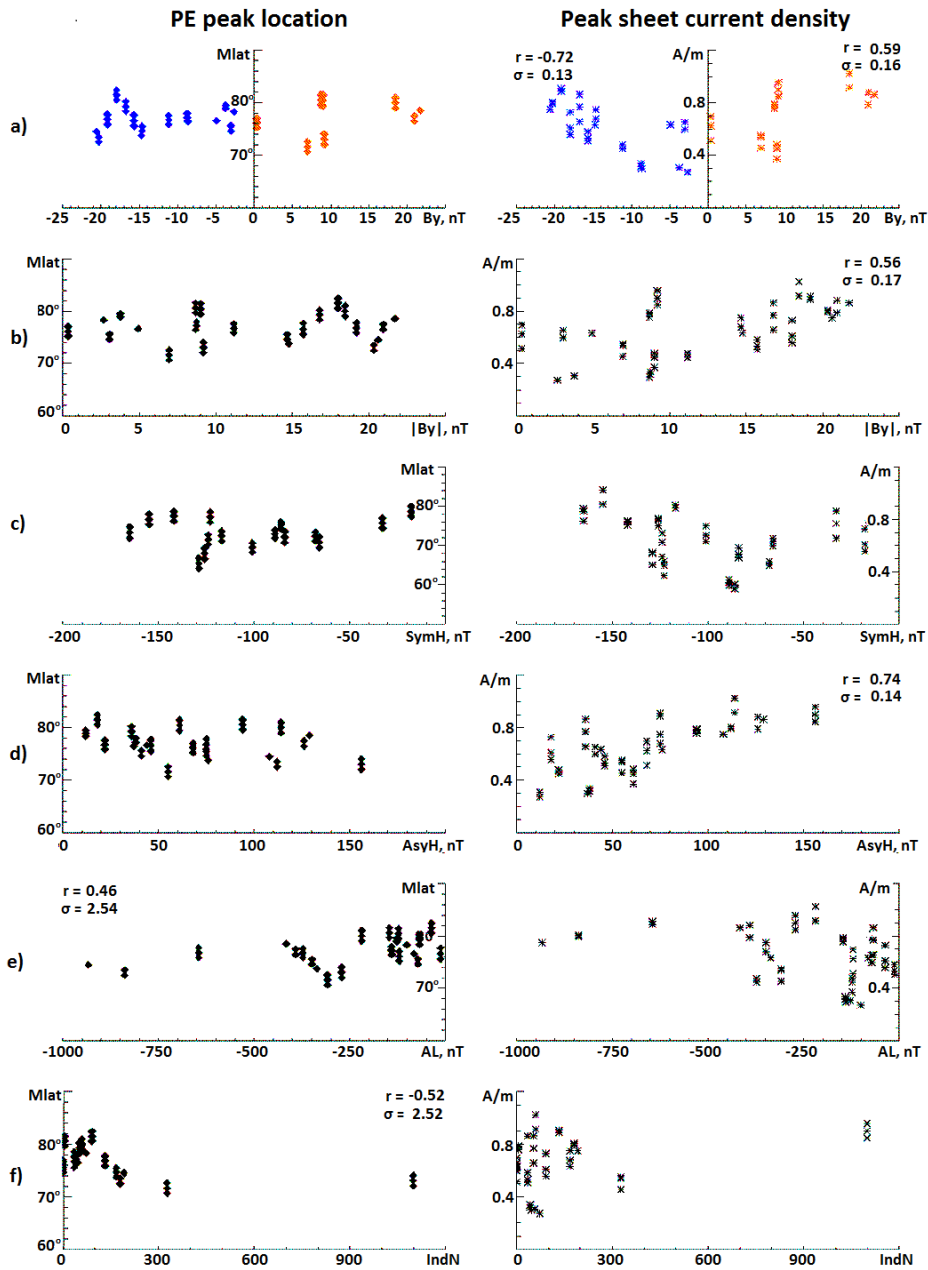
Fig. 3. Dependence of the magnetic latitude MLat (degrees) position of the peak (left column) and its intensity (I in A/m, right column) of the Hall current in the polar electrojet (PE) on the IMF By component (a) and its magnitude (b), on the geomagnetic activity indices SymH (c), AsyH (d), AL (e), and the solar wind coupling function IndN (f). The blue and red data points indicate westward and eastward currents, respectively. For the cases of correlations with $r > 0.46$, the correlation coefficients (r) and the dispersion (σ) according to a linear regression are shown as labels.
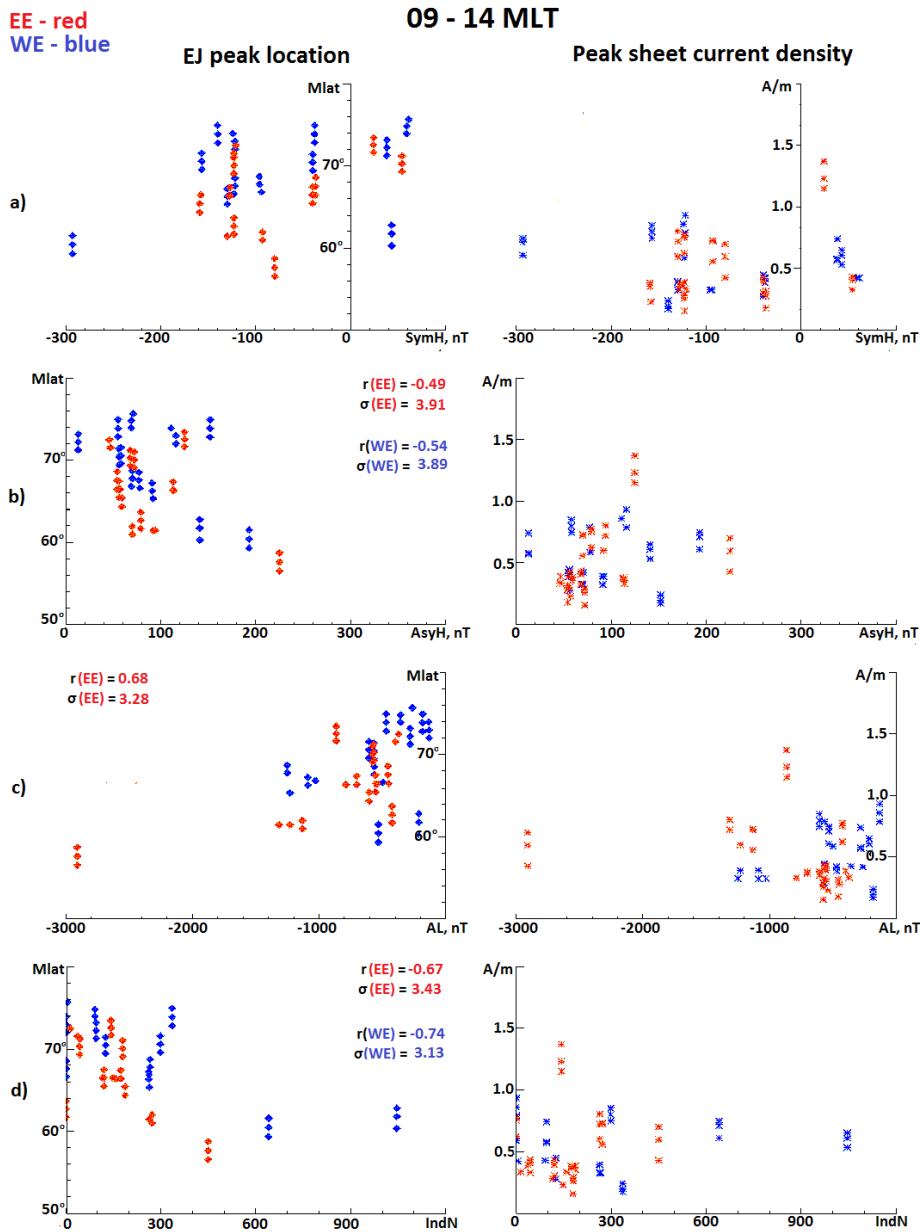
Fig. 4. Daytime sector (09–14 MLT): Dependence of the magnetic latitude MLat (degrees) position of the peak (left column) and of the intensity (I in A/m, right column) of Hall current in the WE (blue) and EE (red) on the geomagnetic activity indices SymH (a), AsyH (b), AL (c), and the solar wind coupling function IndN (d). For the cases of correlations with $r > 0.46$, the correlation coefficients (r) and the dispersion (σ) according to a linear regression are shown as labels.
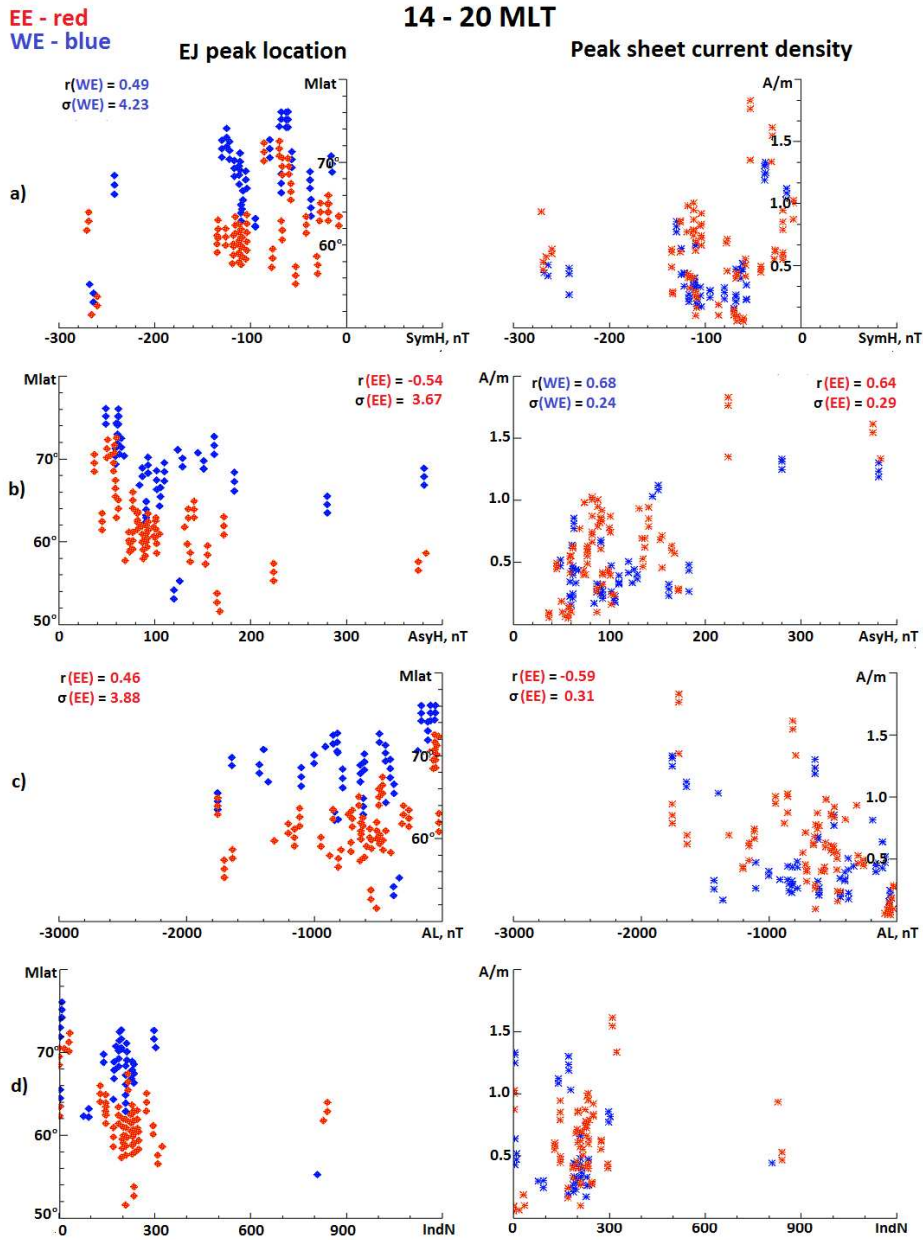
Fig. 5. The same as in Fig. 4, but for the evening sector (14–21 MLT).
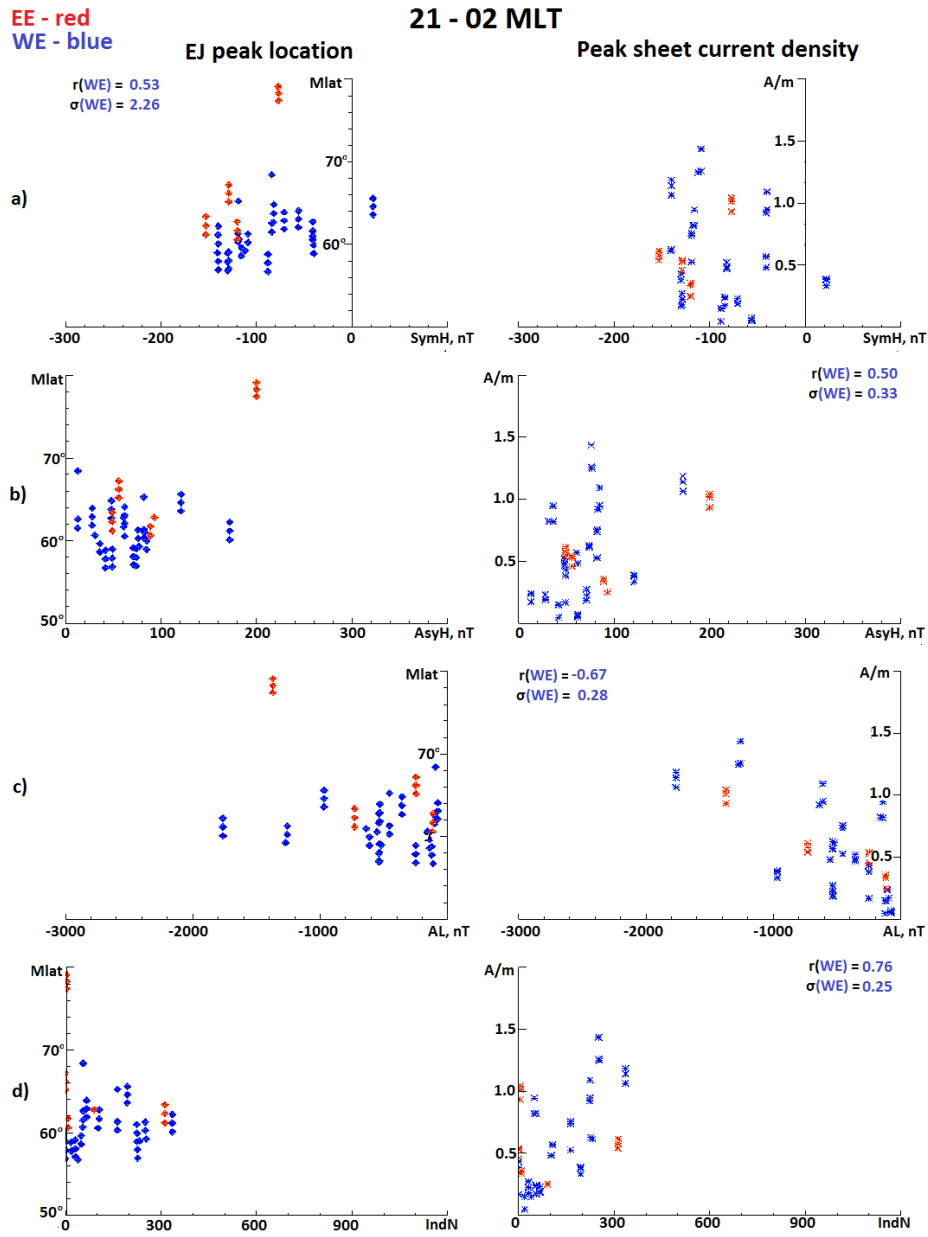
Fig. 6. The same as in Fig. 4, but for the midnight sector (21–02 MLT).
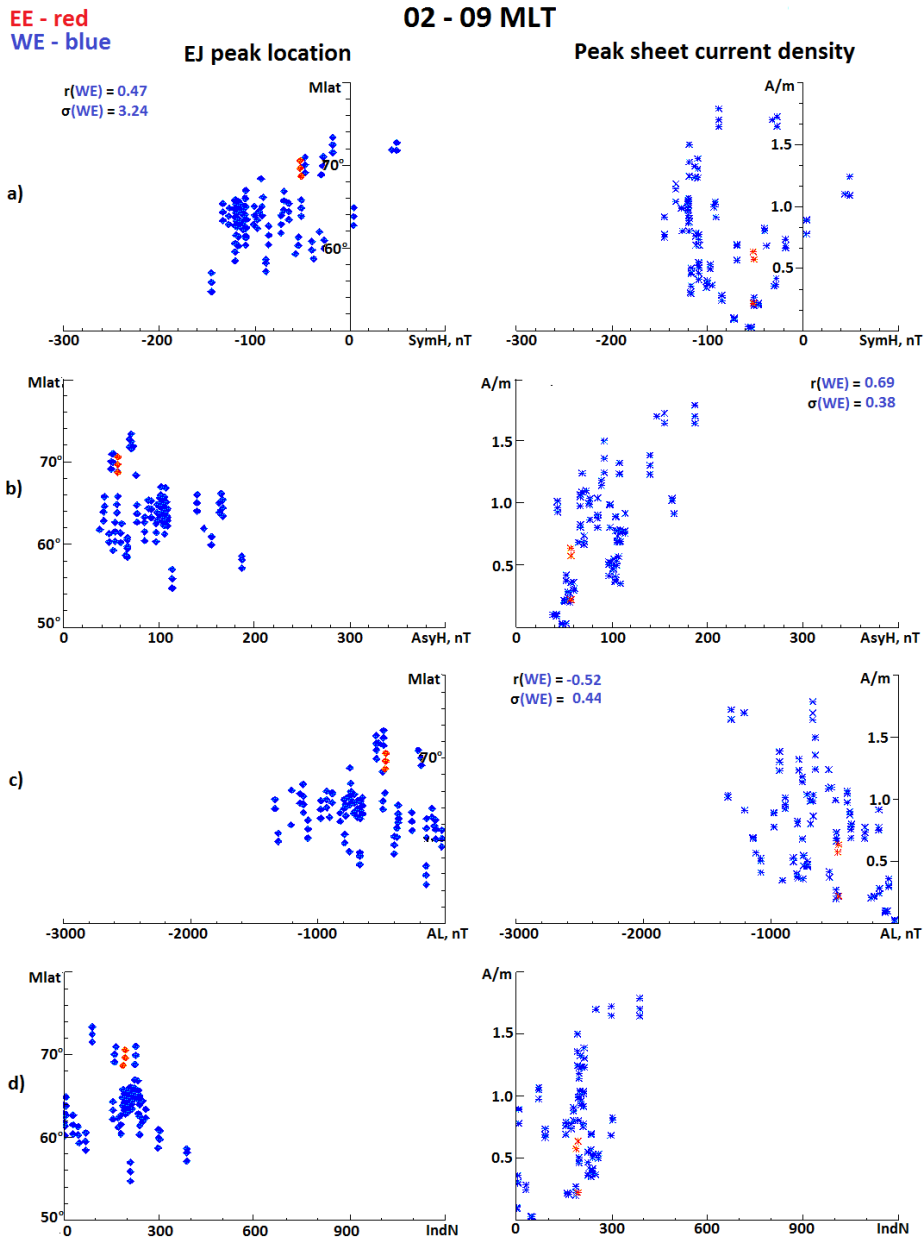
Fig. 7. The same as in Fig. 4, but for the morning sector (02–09 MLT).

2005, Aug 24
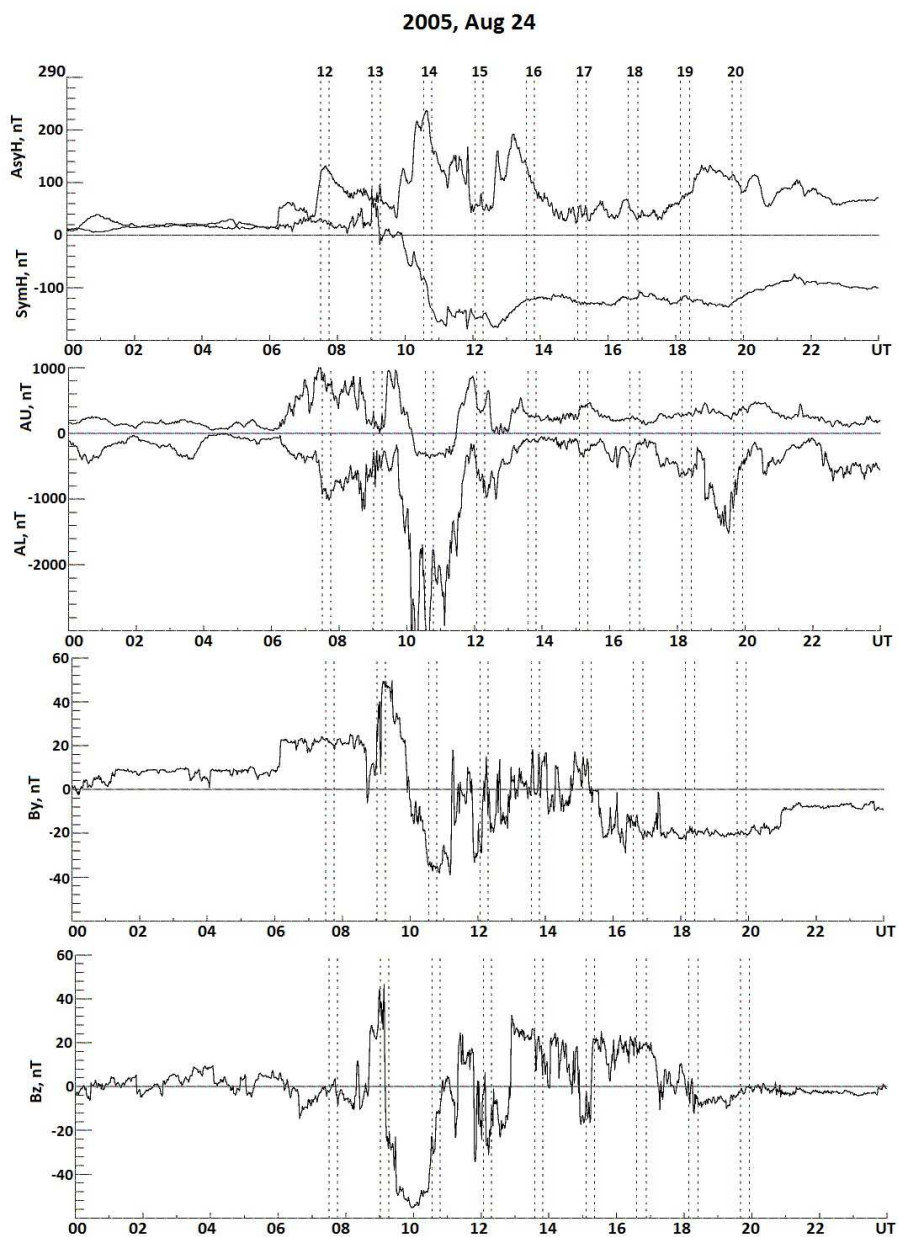
Fig. A1.1. One-minute values of the AsyH, SymH, AU, and AL indices and of the By and Bz components of the IMF for the storm of 24 Aug 2005 (analysis interval from 07:00–20:00 UT, orbits 29012–29020). The time of each orbit and its orbit number are indicated as in Fig. 1 of the paper.
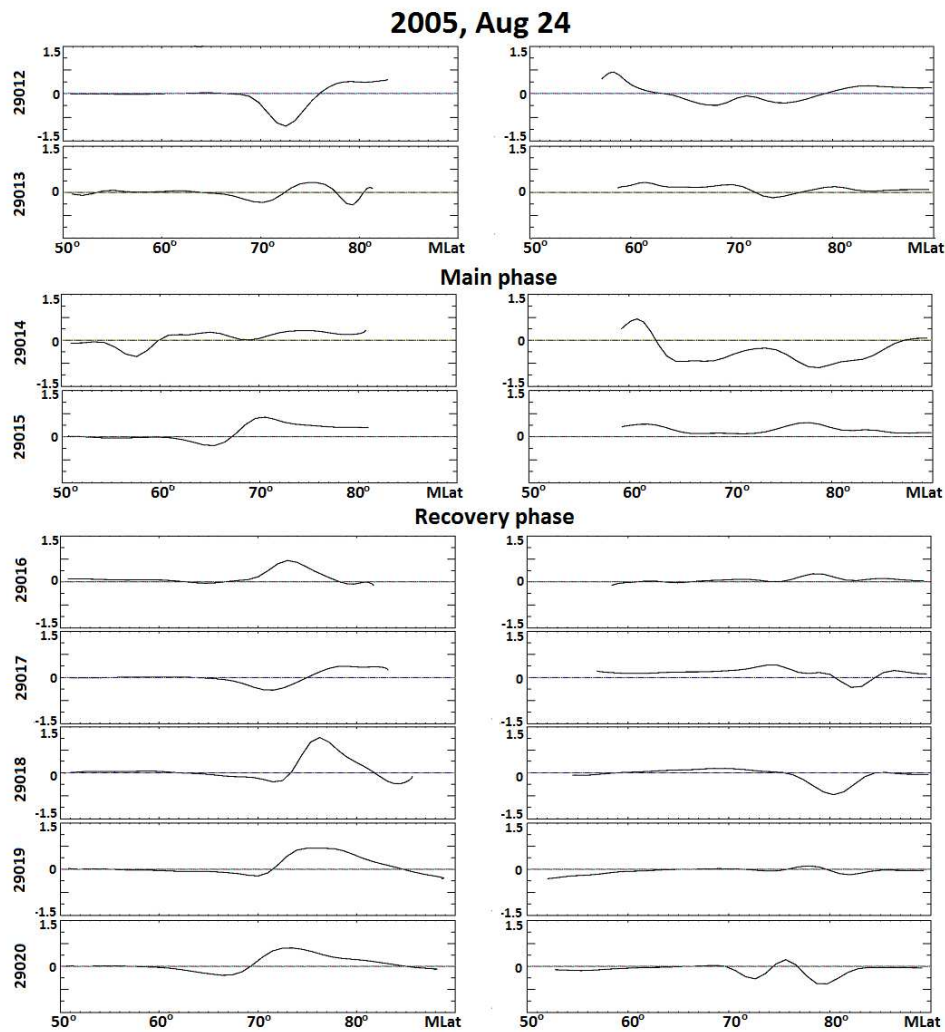
Fig. A1.2. Direction and intensity values of the Hall current along the satellite orbit at the dayside (left column, 11–13 MLT, corresponding to the ascending section of the orbit) and nightside sectors (right column, 23–24 MLT, descending orbit section). Positive currents denotes eastward current for the descending orbit section, and westward current for the ascending section, respectively.

2003, June 18
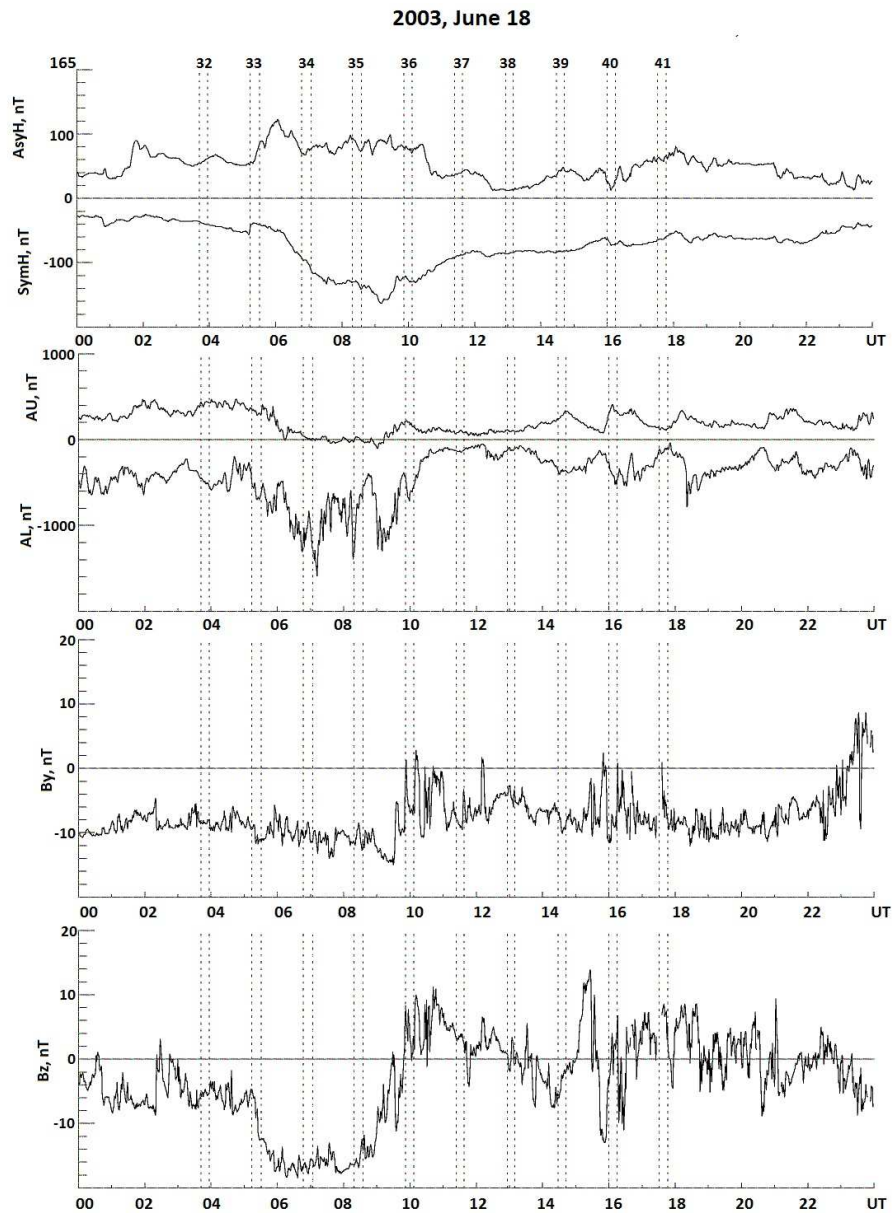
Fig. A2.1. One-minute values of the AsyH, SymH, AU, and AL indices and of the By and Bz components of the IMF for the storm of 18 June 2003 (analysed interval from 03:00–18:00 UT, orbits 16532–16541). The time of each orbit and its orbit number are indicated as in Fig. 1 of the paper.
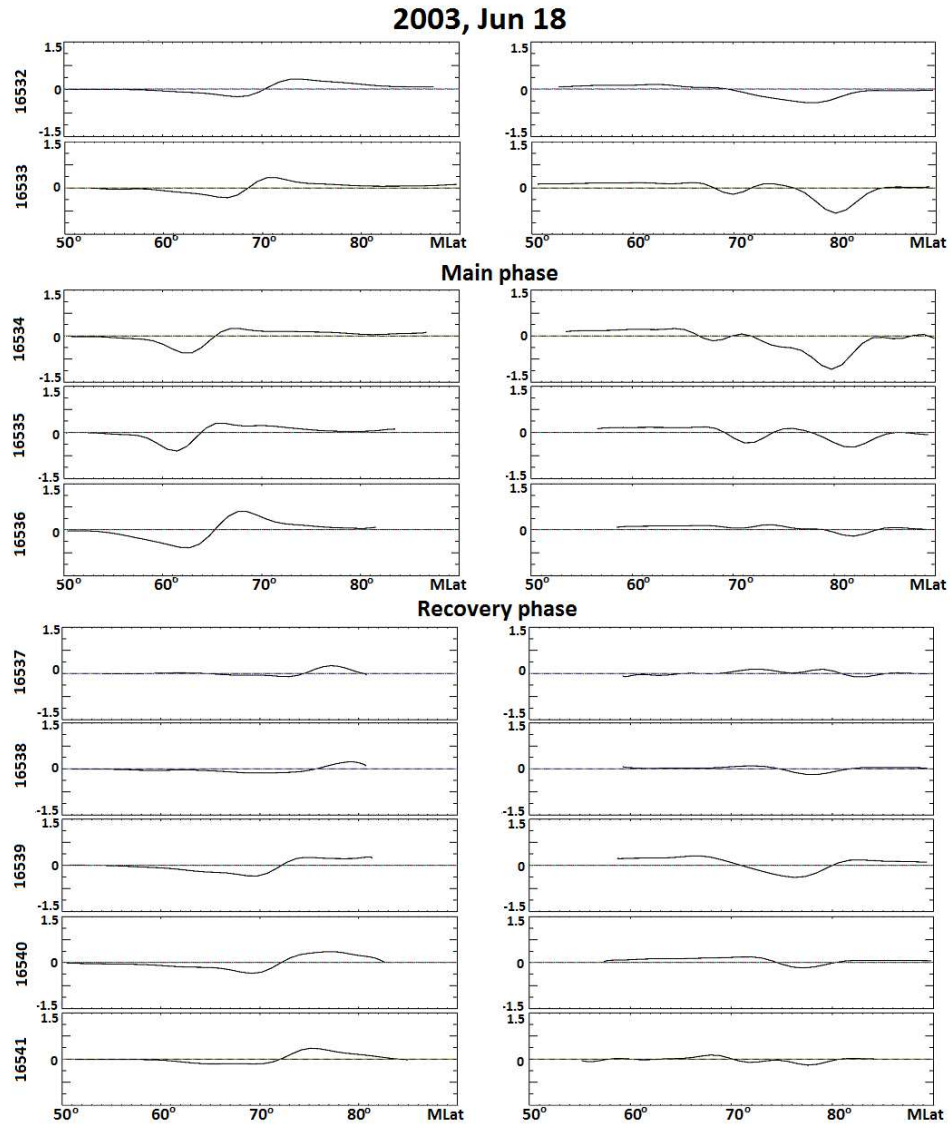
Fig. A2.2. Direction and intensity values of the Hall current along the satellite orbit at the dayside (left column, 12–16 MLT, corresponding to the ascending section of the orbit) and nightside sectors (right column, 00–04 MLT, descending orbit section). Positive currents denotes eastward current for the descending orbit section, and westward current for the ascending section, respectively.
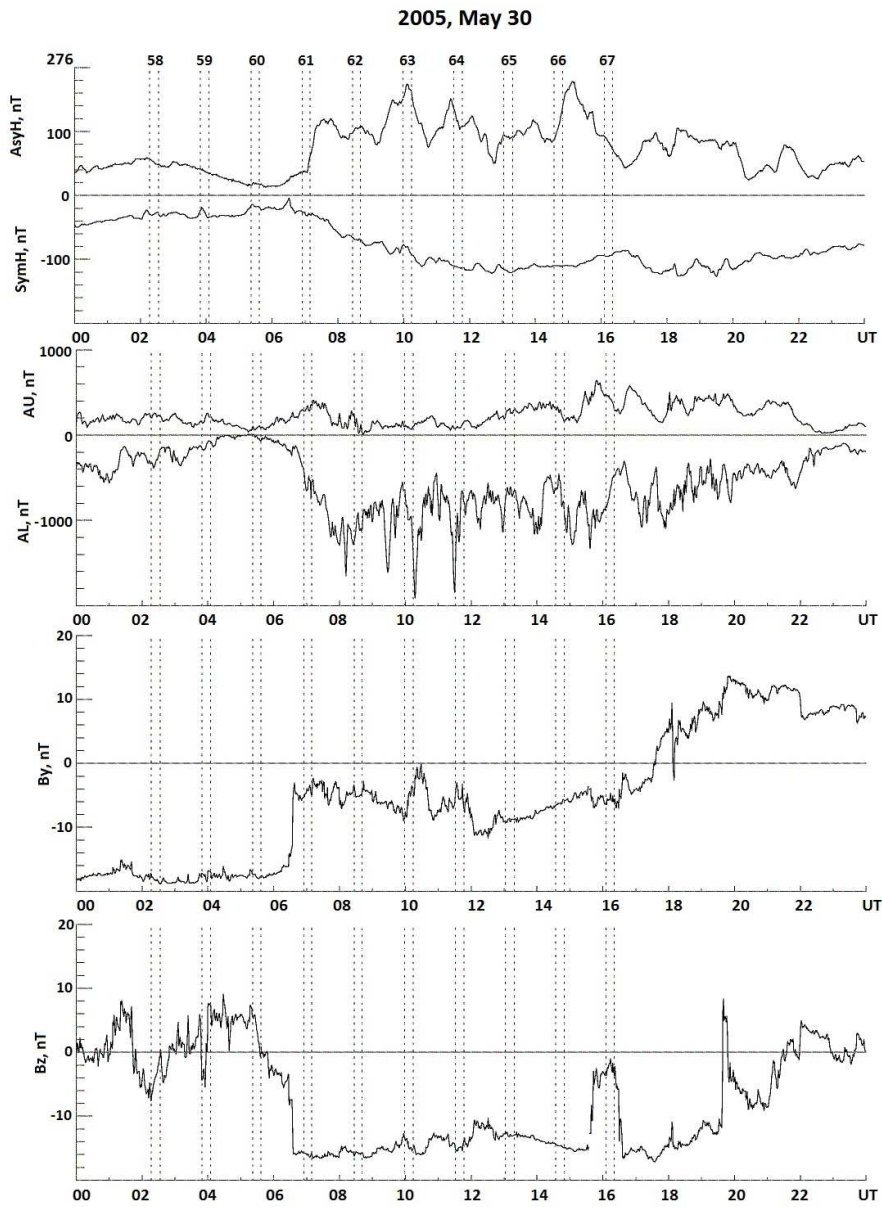
Fig. A3.1. One-minute values of the AsyH, SymH, AU, and AL indices and of the By and Bz components of the IMF for the storm of 30 May 2005 (analysis interval 02:00–17:00 UT, orbits 27658–27667). The time of each orbit and its orbit number are indicated as in Fig. 1 of the paper.
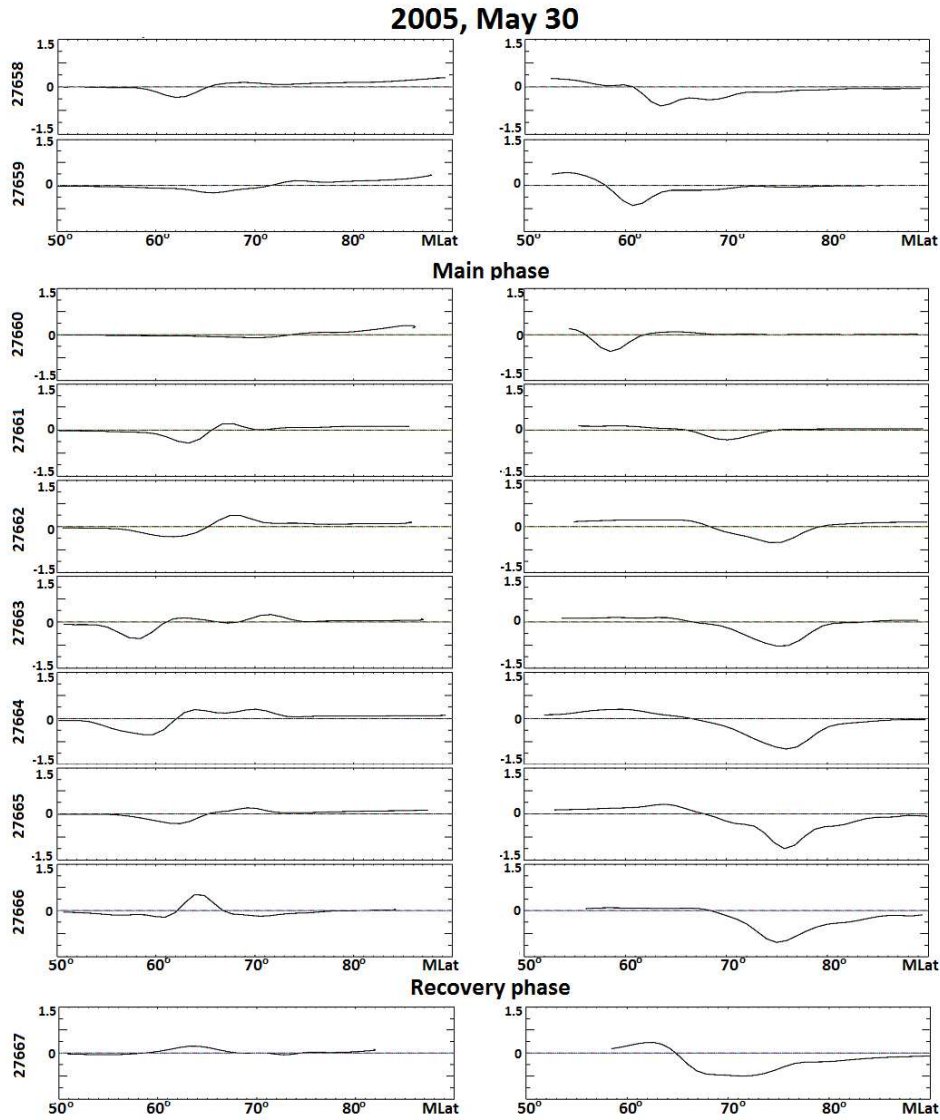
Fig. A3.2. Direction and intensity values of the Hall current along the satellite orbit at the duskside (left column, 19–21 MLT, corresponding to the ascending section of the orbit) and dawnside sectors (right column, 06–09 MLT, descending orbit section). Positive currents denote an eastward current flow for the descending orbit section, and westward current for the ascending section, respectively.
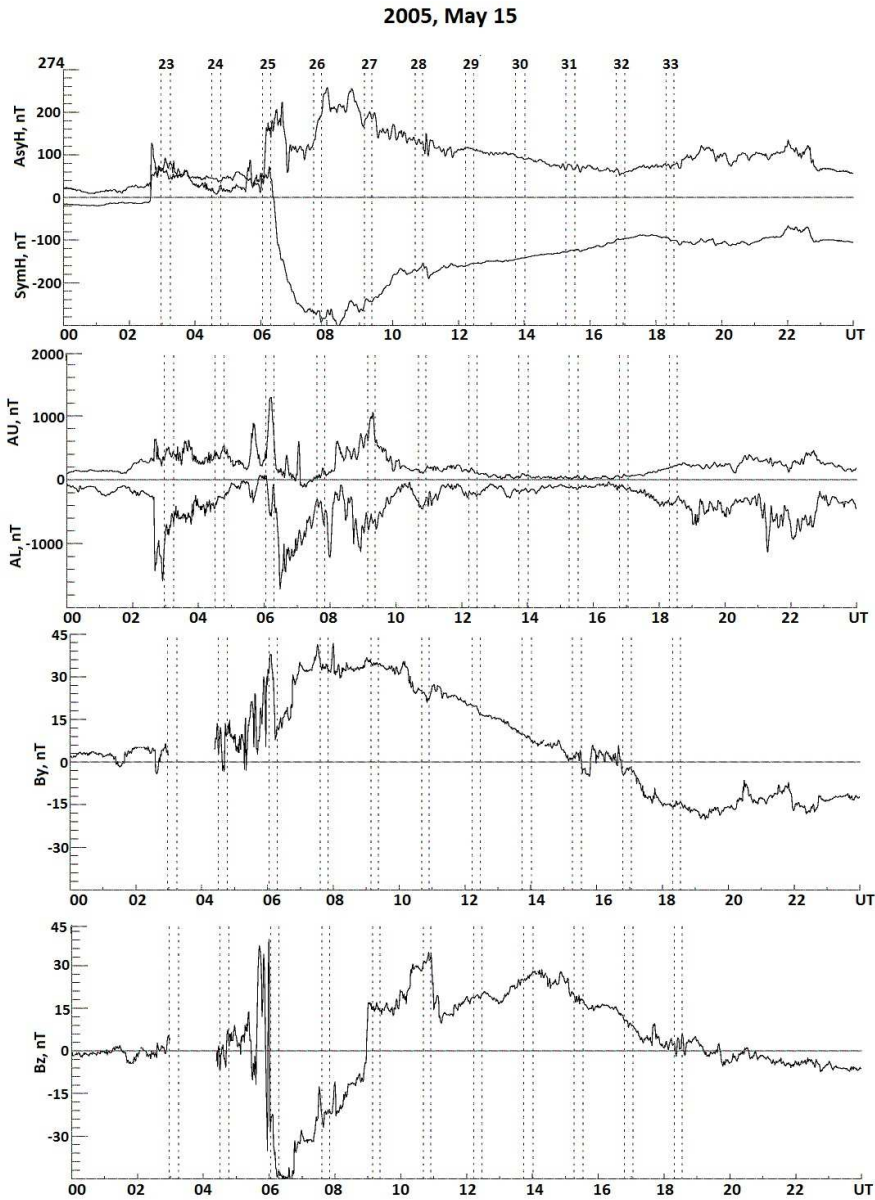
Fig. A4.1. One-minute values of the AsyH, SymH, AU, and AL indices and of the By and Bz components of the IMF for the storm of 15 May 2005 (analysis interval 02:00–19:00 UT, orbits 27423–27433). The time of each orbit and its orbit number are indicated as in Fig. 1 of the paper.
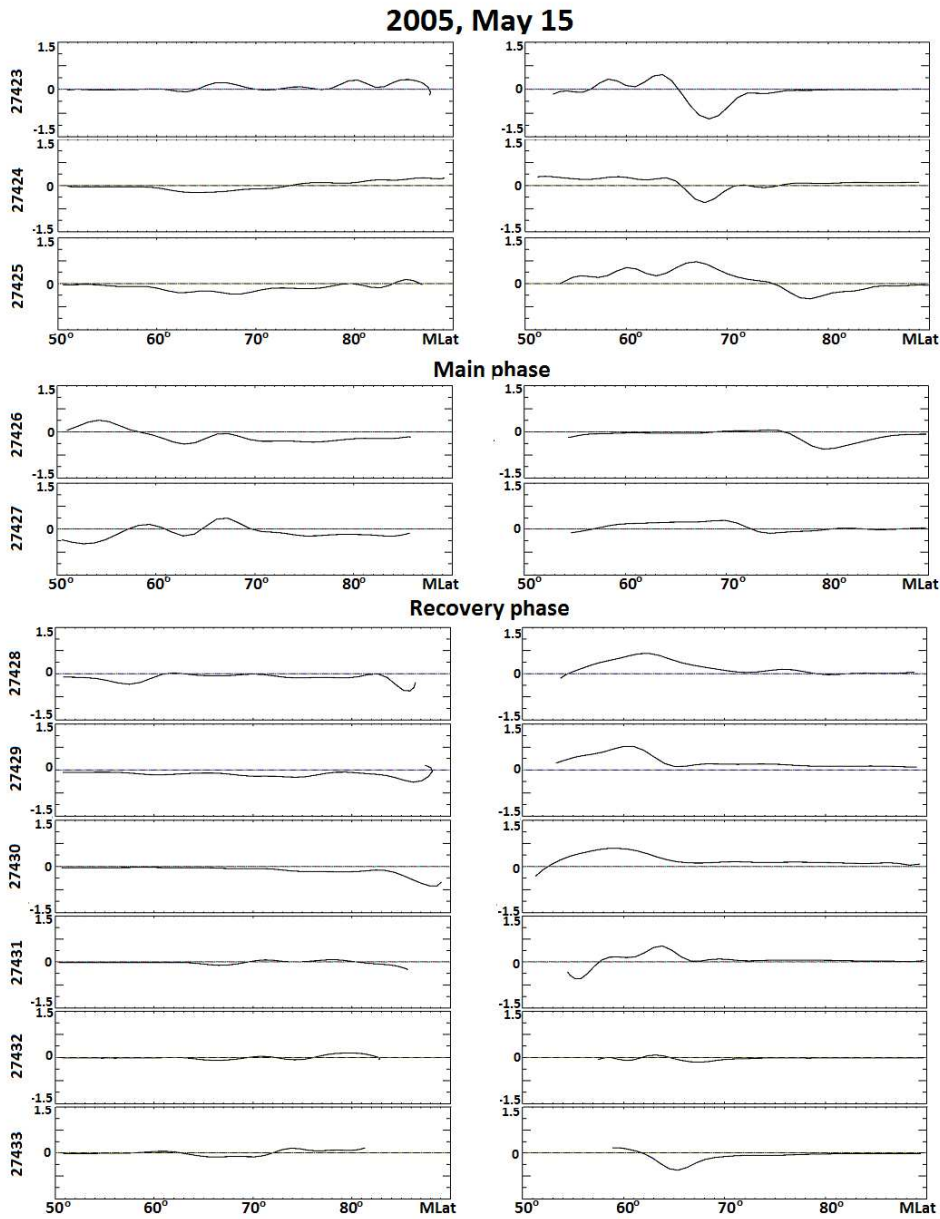
Fig. A4.2. Direction and intensity values of the Hall current along the satellite orbit at the duskside (left column, 20–22 MLT, corresponding to the ascending section of the orbit) and dawnside sectors (right column, 08–10 MLT, descending orbit section). Positive currents denote an eastward current flow for the descending orbit section, and westward current for the ascending section, respectively.
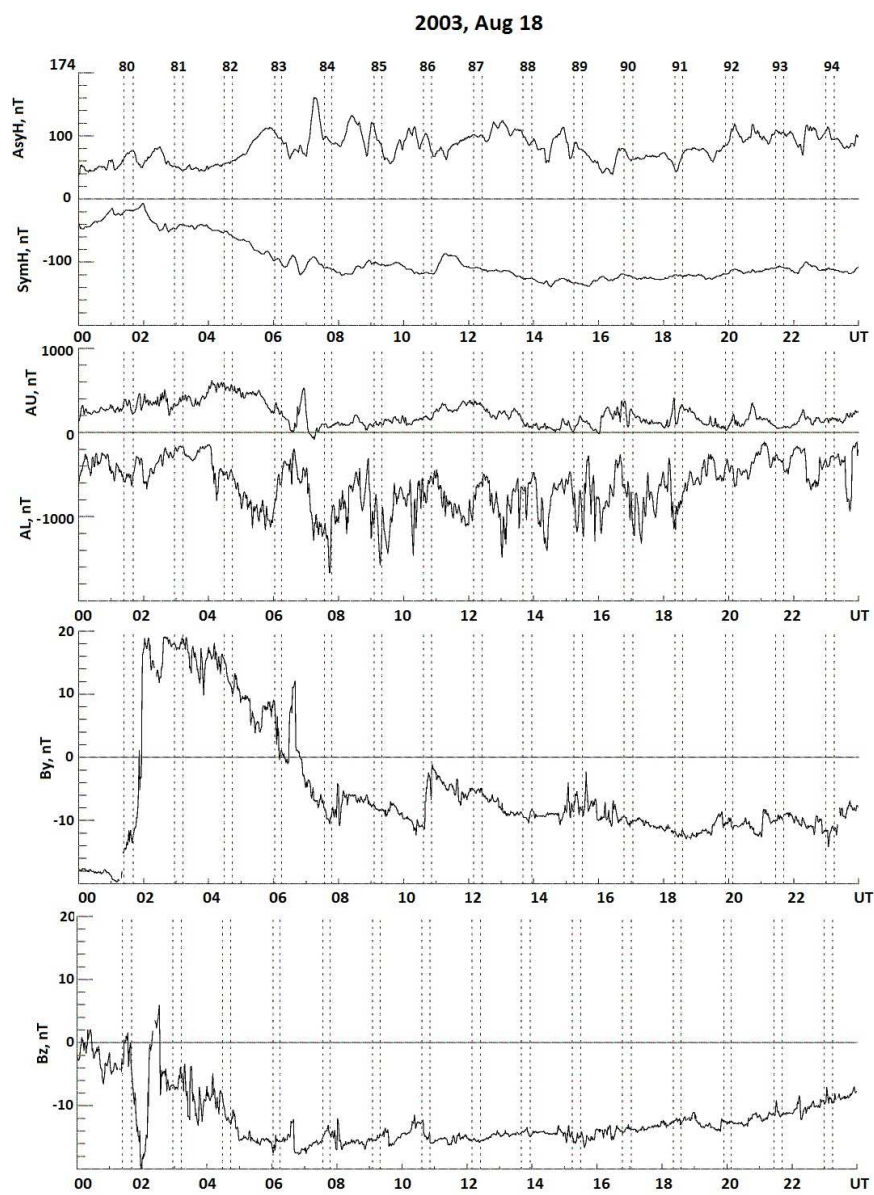
Fig. A5.1. One-minute values of the AsyH, SymH, AU, and AL indices and of the By and Bz components of the IMF for the storm of 18 Aug 2003 (analysis interval 00:00–23:00 UT, orbits 17480–17494). The time of each orbit and its orbit number are indicated as in Fig. 1 of the paper.

2003, Aug 18
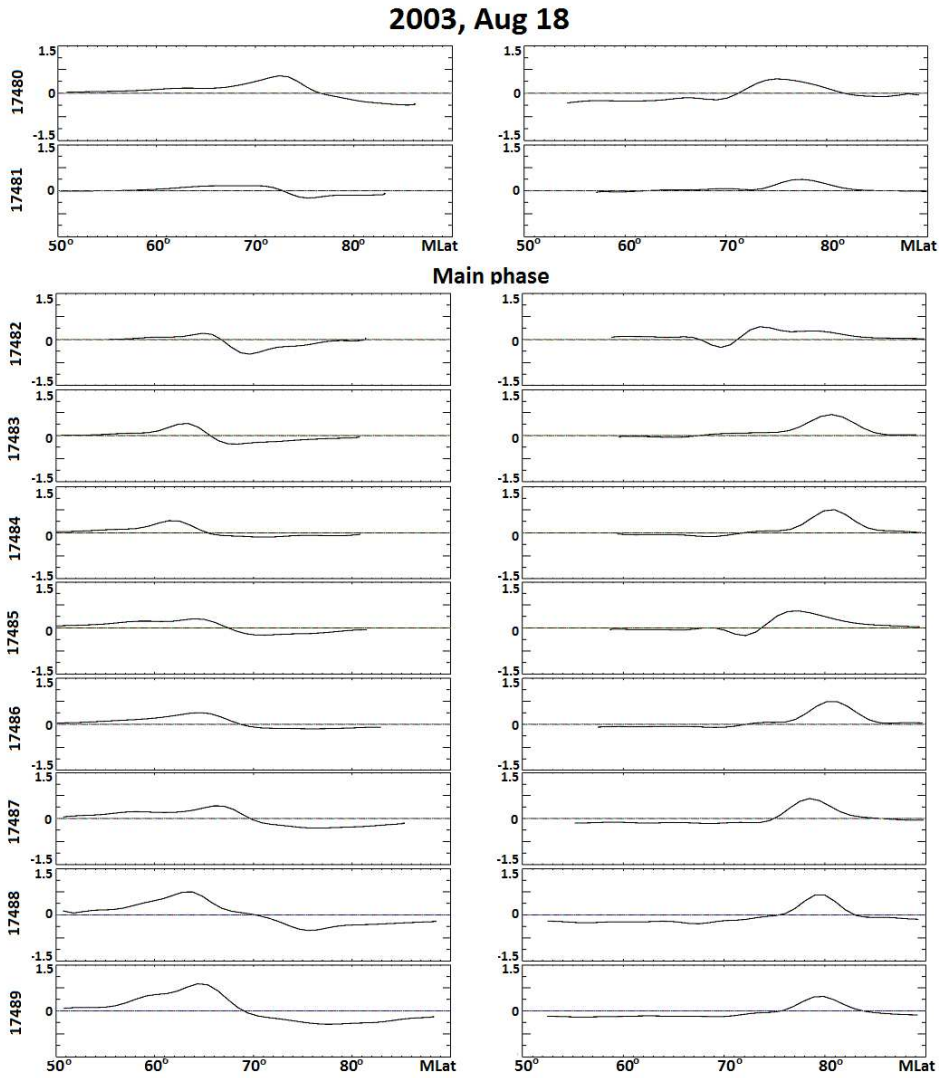
Fig. A5.2. Direction and intensity values of the Hall current along the satellite orbit at the dawnside (left column, 07–09 MLT, corresponding to the ascending section of the orbit) and duskside sectors (right column, 19–21 MLT, descending orbit section). Positive currents denote an eastward current flow for the descending orbit section, and westward current for the ascending section, respectively.